Molecular Phylogenetics and Evolution 214 (2026) 108455

Contents lists available at ScienceDirect

Molecular Phylogenetics and Evolution

journal homepage: www.elsevier.com/locate/ympev

Contrasting diversification patterns across wood rushes from *Luzula* sect. *Luzula* (Juncaceae) revealed by 3RAD genome-wide sequencing

Carolina Carrizo García [a,b], Valentin Heimer [c,d], Peter Schönswetter [c], Claudio Varotto [a], Božo Frajman [c,*], Mingai Li [a,*]

[a] Centro Ricerca e Innovazione, Fondazione Edmund Mach, Via Mach 1, 38098 San Michele all'Adige, Italy
[b] Instituto Multidisciplinario de Biología Vegetal (CONICET-UNC), Av. Vélez Sarsfield 1611, 5000 Córdoba, Argentina
[c] Department of Botany, University of Innsbruck, Sternwartestraße 15, 6020 Innsbruck, Austria
[d] Institute for Alpine Environment, Eurac Research, Drususallee 1/Viale Druso 1, 39100 Bozen/Bolzano, Italy

ARTICLE INFO

Keywords:
3RADseq
Agmatoploidy
Diversification
Luzula
European Alpine System

ABSTRACT

Among the different mechanisms triggering diversification processes, chromosomal rearrangements that generate karyotypic changes are common in plants. *Luzula* (Juncaceae) is among the few angiosperm genera with holocentric chromosomes, which can undergo chromosome fission (agmatoploidy) or fusion (symploidy), resulting in karyotypes with different chromosome numbers and sizes. In this study, 3RAD genome-wide sequencing data and plastid sequences were used to explore evolutionary trends and patterns of genetic diversification among diploid taxa of *Luzula* sect. *Luzula* centred in the European Alpine System. In addition, we inferred its phylogenetic relationships to other closely related sections, of which several proved to be non-monophyletic. The species of *Luzula* sect. *Luzula* are segregated into three lineages, which show contrasting patterns regarding bifurcated branching, reticulation, and levels of coancestry as a result of different evolutionary histories. Agmatoploid species are found in two of these clades, displaying different karyotypes, while the third lineage comprises only *L. campestris*. Based on a molecular dating reconstruction, at least two putatively independent transitions towards agmatoploidy are estimated, which have occurred between the mid- and late Pleistocene in *Luzula sect. Luzula*. In addition, several trans-continental migrations, e.g. between Europe and Africa, were inferred. This study provides a new perspective on the complexity of diversification among wood rushes, which may serve as a basis for future exploration of the occurrence of agmatoploidy and its role in species diversification.

1. Introduction

Across plant lineages, various processes contribute to species diversification, including ecological adaptation, reproductive isolation, and genomic changes, the latter encompassing both molecular and structural features. Variations in chromosome numbers, such as polyploidy and dysploidy, have implications for both micro- and macroevolutionary processes (Escudero et al., 2018). Holocentric (= holokinetic) chromosomes are unique in that they harbour multiple kinetochores, protein complexes that serve as the attachment site for spindle fibres during cell division; in contrast to the "normal type" of monocentric chromosomes, where spindle microtubules attach to a single kinetochore during mitosis or meiosis, in holocentric chromosomes they attach along the whole length through diffuse kinetochores and their fragmentation is thus not necessarily deleterious as the fragmented parts are successfully segregated in daughter nuclei (Hipp et al., 2010; Bureš et al., 2013; Hultén, 2013). In organisms with holokinetic chromosomes, changes in chromosome number and structure are particularly common (Bureš et al., 2013; Escudero et al., 2018). In addition to fragmentation of single or few chromosomes that is most common in organisms with holocentric chromosomes, concerted fission (agmatoploidy) or fusion (symploidy) of complete chromosome sets is also possible (Luceño and Guerra, 1996; Guerra, 2016). The holocentric nature of chromosomes is considered to influence speciation and genomic evolution as it affects genome structure and recombination rates (Escudero et al., 2016; Hofstatter et al., 2022; Zedek et al., 2025). In angiosperms, only about 220 species from five lineages have been reported to possess holocentric chromosomes (Melters et al., 2012), but they are likely more common (Zedek and

* Corresponding authors.
E-mail addresses: Bozo.Frajman@uibk.ac.at (B. Frajman), mingai.li@fmach.it (M. Li).

https://doi.org/10.1016/j.ympev.2025.108455
Received 27 May 2025; Received in revised form 18 August 2025; Accepted 26 August 2025
Available online 2 September 2025

Bureš, 2018). Remarkably, a number of genera of the two sister families Cyperaceae and Juncaceae display holocentricity (Arante Chaves et al., 2024; Bozek et al., 2012; Escudero et al., 2016; Melters et al., 2012), which is, however, absent in the monocentric genus *Juncus* (Juncaceae; Mata-Sucre et al., 2023). On the other hand, its sister genus *Luzula*, encompassing ca. 115 species worldwide, is characterized by holocentric chromosomes. *Luzula* is the only known plant group where simultaneous fragmentations of complete chromosome sets were evidenced, whereas in other taxa only partial agmato- and/or symploidy has been documented (Guerra, 2016). Agmatoploidy and symploidy, along with true polyploidy, contributed to a wide karyotypic diversity and thus to the diversification of *Luzula* (Bozek et al., 2012), where three chromosome sizes are known: AL-type are the largest, full-size chromosomes, BL-type are intermediate, half-size chromosomes, and CL-type are the smallest, quarter-size chromosomes (Nordenskiöld, 1951; Bozek et al., 2012). In addition, exceptionally long chromosomes referred to as > AL-type, probably resulting from symploidy, have been reported for two species (Bozek et al., 2012). The most common and putatively ancestral karyotype in *Luzula* is $2n = 12$AL (Bozek et al., 2012), but underlying phylogenetic studies enabling ancestral karyotype reconstruction are missing.

The current knowledge of *Luzula* diversity relies on several regional studies (e.g., Edgar, 1966; Kirschner and Křisa, 1979; Kirschner, 1996) resulting in a comprehensive taxonomic monograph (Kirschner, 2002). Nevertheless, a number of species have been described more recently and their exact distributions remain unknown (Bačič et al., 2007, 2016, 2019; Kirschner, 2007). In addition, infrageneric phylogenetic relationships based on ITS and plastid sequences were poorly resolved, in particular within monophyletic *Luzula* sect. *Luzula* (Bozek et al., 2012; Drábková et al., 2006; Záveská Drábková and Vlček, 2009, 2010; Brožová et al., 2022). This section is the most variable and taxonomically diverse group within the genus, with Europe being one of its diversity centres (Kirschner, 2002; Drábková et al., 2003). Most species in Europe, about ten, occur in the central parts of the European Alpine System (EAS; Ozenda, 1985), specifically in the Alps and adjacent areas. They include diploids with AL-, BL- and CL-type chromosomes as well as tetra- and hexaploids (Kirschner, 2002; Aeschimann et al., 2004; Bačič et al., 2007, 2019). The species of this group are characterized by morphological similarity and partly shared habitats, ranging from lowlands to alpine grasslands (Kirschner, 2002; Bačič et al., 2019; Pungaršek et al., 2023), making them suitable for studying the diversification and evolutionary relationships among closely related species, in particular in relation to their karyotypic variability. Different hypotheses on the diversification of *Luzula* sect. *Luzula* and the putative origin of agmatoploid and polyploid taxa have been proposed based on karyological and morphological, and, to a lesser extent, molecular data (Kirschner, 1992, 2002; Bačič et al., 2019; Pungaršek et al., 2023). However, incomplete taxonomic and geographic sampling and lack of phylogenetic resolution in previous studies left several questions unanswered, especially regarding the origin of agmatoploid species. While it is established that polyploids can form repeatedly in flowering plants (Soltis et al., 2016), it remains unclear whether synchronized chromosome fissions are likely to happen multiple times, thus leading to recurrent formation of agmatoploids from different populations of the same parental species.

In this study, we used SNP markers obtained through a modified double-digest restriction-site associated DNA sequencing as well as plastid sequences to infer diversification across diploid taxa of *Luzula*, and especially *Luzula* sect. *Luzula*, with a geographical focus on the EAS. In particular, we disentangle the origin of agmatoploids and assess whether they were formed once or multiple times. We examine the underlying patterns of genetic diversity and divergence in a spatio-temporal context and infer genome size evolution across lineages. Ultimately, our study provides novel information about distribution patterns and species delimitations within *Luzula* sect. *Luzula* in Europe and establishes a phylogenetic backbone among several other sections of *Luzula*.

2. Materials and methods

2.1. Plant material and identification of samples

We focused our sampling on diploid (including agmatoploid) species of *Luzula* sect. *Luzula* native to the EAS and adjacent areas, plus one species from the Caucasus and two from Africa (Table S1, Fig. 1). In addition, we included twelve diploid species from four other sections of *Luzula* and *Juncus effusus* as close and distant outgroups, respectively (Table S1). We sampled one to two individuals per population, i.e., sampling locality, totalling 171 individuals from 21 *Luzula* species and two individuals of *J. effusus*. Maps of sampling localities (Figs. 1, S1–S3) were created using Open Source QGIS v.3.22.4. Leaf material for each sample was harvested and preserved in silica gel and herbarium specimens were prepared and deposited at the herbarium IB. As identification of species within *Luzula* sect. *Luzula* is notoriously difficult and their distributions are insufficiently known (Bačič et al., 2019; Pungaršek et al., 2023), we supported our field-identifications based on morphology and ecology (following Bačič et al., 2016, 2019) with relative genome size estimation (see subsection 2.2) to ascertain diploidy of all samples used. In addition, we used published chromosome counts (Bačič et al., 2016, 2019; Table S1) and counted the chromosomes (see subsection 2.2) for six populations (Table S1) to determine the karyotype for a subset of samples. Differentiation between *L. divulgatiformis* ($2n = 24$BL) and *L. taurica* ($2n = 12$AL) in the Balkan and Apennine peninsulas proved to be most difficult, especially since several samples that were morphologically identified as *L. taurica* (and were also phylogenetically close to this species; see Results section) had approximately 24 chromosomes (it was not possible to establish the exact number in some cases). Since Bačič et al. (2016) identified some samples from the Balkan Peninsula with $2n = 24$BL as putative *L. taurica* based on morphology, and hypothesized that occasional fission of chromosomes can occur in this species, we here for simplicity refer to all the samples morphologically resembling this species and phylogenetically close to the *L. taurica* core clade (including samples with $2n = 12$AL; see Results section) as *L.* cf. *taurica*.

2.2. Genome size estimation and chromosome counting

The relative genome size (RGS) of 167 *Luzula* samples (Table S1) was measured following Suda and Trávníček (2006), using *Bellis perennis* (2C = 3.38 pg; Schönswetter et al., 2007) as an internal standard. Briefly, nuclei were extracted from silica dried leaf material through chopping with a razor blade or grinding with glass beads in a tissue lyser (Qiagen) and stained with 4′,6-diamidino-2-phenylindole (DAPI). Relative fluorescence intensity of 3,000 particles was recorded using a CyFlow Space flow cytometer (Sysmex Partec) and analysed in R v.4.3.3 (R Core Team, 2024) using the package flowPloidy (Smith et al., 2018). The RGS was compared among members of *Luzula* sect. *Luzula* to explore interspecific variability. The chromosome number was determined for six individuals from Feulgen-stained and squashed root tips of germinating seeds as described by Bačič et al. (2019).

2.3. Genomic DNA extraction

Total genomic DNA was extracted from silica gel dried leaf tissue (ca. 10 mg) following a modified cetyltrimethylammonium bromide (CTAB) protocol (Tel-Zur et al., 1999) and purified further with the NucleoSpin gDNA clean-up kit (Macherey-Nagel). The concentration of purified genomic DNA was quantified using a Qubit 4 fluorometer (ThermoFisher Scientific).

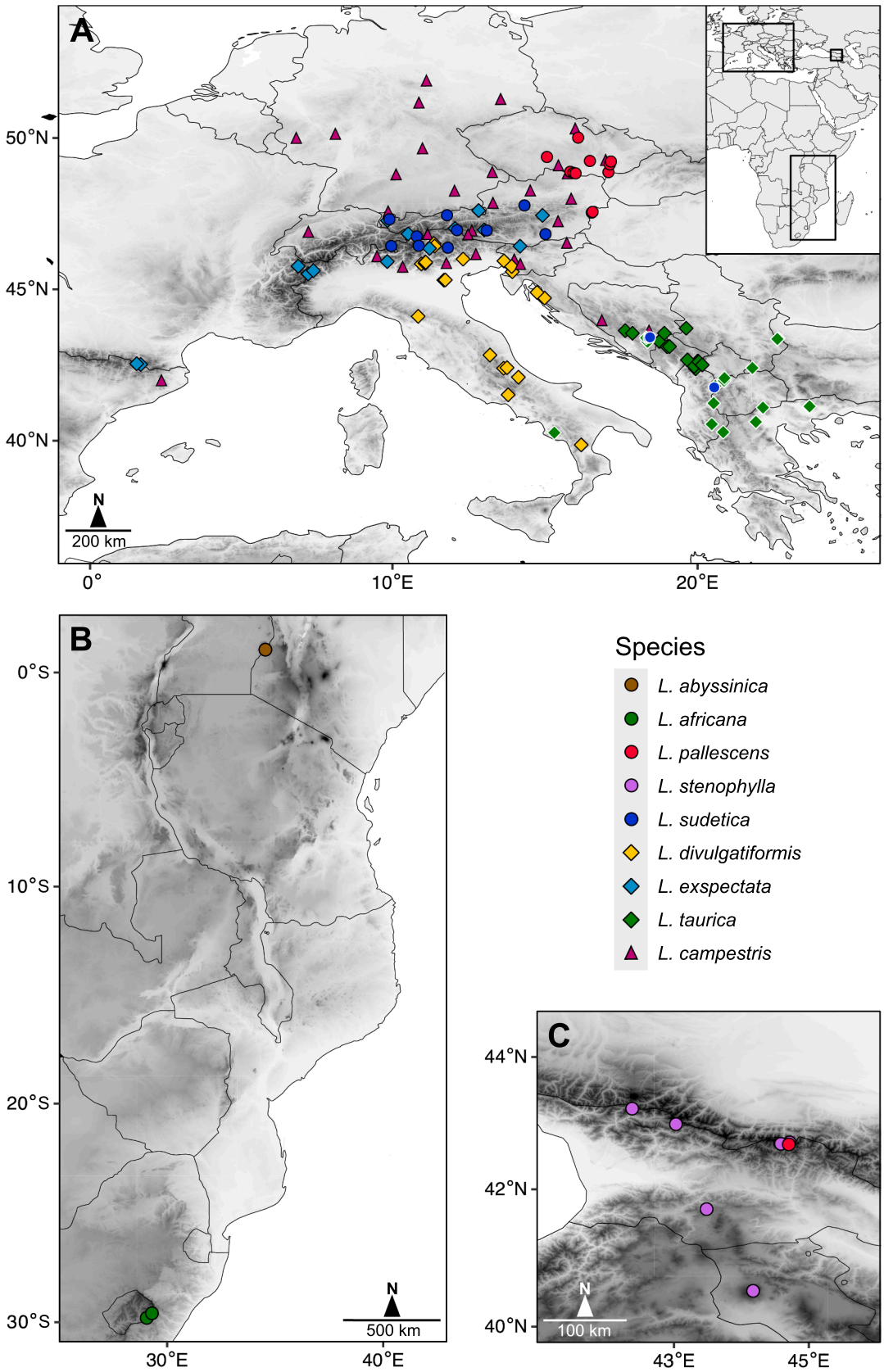

Fig. 1. Distribution of the studied populations of *Luzula* sect. *Luzula* in (A) Europe, (B) eastern Africa, and (C) the Caucasus and southerly adjacent areas. The colours corresponding to taxa as indicated in the legend are used in the same way in all other figures. Samples referred to as *L.* cf. *taurica* and *L.* cf. *sudetica* are indicated with symbols with white margin.

2.4. 3RADseq

2.4.1. 3RADseq library preparation, sequencing, raw reads filtering and locus assembly

The 3RADseq libraries were prepared following the 3RAD method developed by Bayona-Vásquez et al. (2019), employing the restriction enzymes EcoRI, XbaI and NheI (New England Biolabs). This protocol is a modification of a standard ddRADseq protocol that offers several practical advantages such as a simplified workflow and reduced costs, which makes it particularly suitable for processing large numbers of samples (Bayona-Vásquez et al., 2019). Briefly, 100 ng of genomic DNA was digested with EcoRI and XbaI; NheI was used to cut adapter dimers for improved ligation efficiency (Bayona-Vásquez et al., 2019). After ligating unique adapter combinations to the digested DNA, 96 ligation products were pooled and purified using SPRI beads (Beckman Coulter). The purified product was used as a template in a 14-cycle PCR amplification with unique combinations of iTru5 and iTru7 primers. Afterwards, the PCR products were purified with SPRI beads, size-selected for 470–600 bp on BluePippin (Sage Science) and used for Illumina sequencing. The libraries were sequenced with a NovaSeq X Plus at Novogene (Cambridge Science Park), yielding 150-base pair (bp) paired-end reads at a minimal depth of 82.5 Gbp per library.

Demultiplexing of raw reads was done with the process_radtags tool from Stacks v.2.66 (Catchen et al., 2013) and read quality was checked with FastQC v.0.11.9 (Andrews, 2010). The 3RAD sequencing of the 168 samples analysed resulted in ca. 1.1 billion paired-end reads, with 0.2 to 30 (average 6.3) million reads per sample. Demultiplexed reads were processed using ipyrad v.0.9.57 (Eaton and Overcast, 2020) to build datasets for further analysis. Concatenated datasets with different subsets of samples were prepared to perform analyses of (1) general evolutionary trends within *Luzula*, and (2) diversification and shared ancestry within *Luzula* sect. *Luzula* (Table S1). 3RADseq loci were assembled *de novo* in ipyrad with default settings, except for the parameter 21, i.e., the minimum number of samples with data per locus (minsl). Different values were set for this parameter in order to explore the impact of different amounts of missing data. Output files were written in different formats to be further processed according to the specific analysis. All steps from demultiplexing to ipyrad processing, as well as maximum likelihood (ML) tree searches, were carried out in the HPC MACHINA cluster at the Fondazione Edmund Mach (Italy).

2.4.2. Phylogenetic analyses of 3RADseq data

Phylogenetic analyses were performed at two levels: genus-wide, and focused on *Luzula* sect. *Luzula*. The genus-wide analysis was done using ML. The dataset for this analysis consisted of 70 samples from 21 species of *Luzula*, of which 46 belong to nine species of *Luzula* sect. *Luzula*, and the rest to twelve species from four other sections (dataset 1; Table S1). In addition, two samples of *J. effusus* were used for rooting. The *snps* output file (all SNPs) written by ipyrad with 25, 30, 40 and 50 % minsl were subjected to ML analysis in IQ-TREE 2 (Minh et al., 2020). The best-fitting substitution model was determined using BIC in ModelFinder (Kalyaanamoorthy et al., 2017). Branch supports were assessed with 1000 replicates of ultrafast bootstrap approximation (UBoot) implemented in IQ-TREE 2 (Hoang et al., 2018). The topologies inferred from the datasets with four different levels of missing data were highly congruent, with slight differences in topology and support values mostly close to the crown of the trees, where the clades were moderately to weakly supported. Finally, the dataset with 30 % minsl, comprising 32,234 variable sites, was selected since it yielded the best support throughout. The best-fitting model for this dataset was TVMe + ASC + R3.

The in-depth analysis of phylogenetic affinities within *Luzula* sect. *Luzula* (dataset 2) was also performed with a ML analysis in IQ-TREE 2 as described above; minsl was set to 50 % after testing congruence using different values. The dataset assembled with ipyrad consisted of 140 samples belonging to nine species of *Luzula* sect. *Luzula* plus six samples of *L. spicata* used for rooting (Table S1) and included 23,268 variable sites. The best-fitting model chosen according to the BIC was TVMe + ASC + R2.

In addition, we constructed NeighborNets for dataset 2, excluding *L. spicata*, using the uncorrected *p-distance* in SplitsTree v.6.3.27 (Huson and Bryant, 2024). Biallelic SNPs with minor allele frequency (maf) 0.05 were filtered using VCFtools v.0.1.17 (Danecek et al., 2011) from the VCF file produced with ipyrad, setting the maximum proportion of missing data per site to 10, 20 and 30 %. The phylogenetic networks obtained were consistent using any of these percentages; thus only one is presented (maximum 20 % missing data, 2,701 SNPs). Reticulation events were also separately explored within Clade B of *Luzula* sect. *Luzula* (see Results section). The corresponding samples were filtered from the VCF file written in ipyrad. All biallelic SNPs with maf 0.05 and a maximum of 20 % of missing data per site were retained (2,032 SNPs) to build a NeighborNet.

2.4.3. Divergence time estimation

Divergence times were estimated using SNAPP (Bryant et al., 2012). To reduce computational demand, one or two individuals were selected from each *Luzula* species (or monophyletic group for paraphyletic species; see Results section), constituting dataset 3. Biallelic SNPs were filtered for 39 selected individuals (Table S1) and, to reduce linkage between the SNPs, the dataset was thinned with VCFtools to keep one SNP every 100 bp. A custom ruby script (https://github.com/mmatschiner/snapp_prep/blob/master/snapp_prep.rb) was used to prepare the input xml file to run SNAPP in BEAST2 v.2.7.7 (Bouckaert et al., 2019). Finally, only SNPs without missing data across species were selected, resulting in a dataset of 286 biallelic independent SNPs. The monophyly of *Luzula* sect. *Luzula* and of the major Clades A and B (see Results section) was fixed. A secondary calibration point was set at 4 Ma (lognormal; standard deviation of 0.1) for the split between *L. spicata* and *Luzula sect. Luzula* based on Elliot et al. (2024). The ML tree obtained for the entire genus (dataset 2) was adapted and provided as the starting tree to initiate the MCMC chain. Two independent runs were done in BEAST2 for 950,000 and 1,000,000 generations, sampling every 500 generations. BEAST2 was run on the CIPRES Science Gateway (Miller et al., 2010). The log files were analysed in Tracer v.1.7.2 (Rambaut et al., 2018) to test convergence; the effective sample size (EES) was > 200 for all parameters. Tree files were combined with LogCombiner v.2.7.7 (Bouckaert et al., 2019) discarding 10 % of trees as burn-in. The maximum credibility tree/chronogram of mean heights was built using TreeAnnotator v.2.7.7 (Bouckaert et al., 2019) and plotted in FigTree v.1.4.4 (Rambaut, 2018).

2.4.4. Analyses of genetic structure and admixture in Luzula sect. Luzula

Shared ancestry among individuals of *Luzula* sect. *Luzula* was estimated with fineRADstructure (Malinsky et al., 2018). Datasets were written using ipyrad (*alleles* format) and 25, 30 and 50 % of minimum samples per locus were tested. For each of the three datasets, co-ancestry matrices were generated with RADpainter and then individuals were assigned to populations using the fineSTRUCTURE MCMC clustering algorithm (sampling 100,000 iterations after 10,000 iterations as burn-in). A tree was built with fineSTRUCTURE. The co-ancestry matrices and the coalescence trees for each dataset analysed were plotted in R using the script fineRADstructurePlot.R (Malinsky et al., 2018). The results were congruent across different percentages of missing data applied, therefore only the result for 25 %, which produced the best-defined groups, is shown.

Genetic structure was also analysed within Clade B of *Luzula* sect. *Luzula* (see Results section), incorporating the spatial dimension. Biallelic SNPs with maf 0.05 and 20 % maximum number of sites with missing data were filtered using VCFtools. SNPs were further filtered to keep only the first SNP per locus with the vcf_parser.py script (part of the RAD Tools collection at https://github.com/CoBiG2/RAD_Tools/tree/master). This dataset included 638 SNPs and was analysed using tess3r

(Caye et al., 2016), which integrates the geographic location of the samples and uses algorithms based on least-squares optimization and on geographically constrained non-negative matrix factorization (Caye et al., 2016). The function tess3 was applied with the following parameters: K = 1:10, rep = 10, iterations = 100, method = projected.ls, and ploidy = 2. The cross-entropy criterion was used to evaluate the best number of ancestral populations (K).

2.5. Evolutionary reconstruction of relative genome size

Reconstruction of ancestral character states for the RGS across *Luzula* was done in R. The ML tree obtained with dataset 1 was used as input after pruning samples with no RGS data available with the drop.tip function of the ape package (Paradis and Schliep, 2019). The phylogenetic signal was estimated with the phylosig function of the phytools package (Revell, 2024) using Pagel's λ method (Pagel, 1999). The best-fitting model of character evolution was selected by comparatively analysing the likelihood of the Brownian motion (BM), Ornstein-Uhlenbeck (OU) and Early-burst (EB) models using the fitContinuous function of the geiger package (Pennell et al., 2014). Akaike weights were computed with the aic.w function of phytools to select the model with the best fit, which was EB. Ancestral states of RGS were reconstructed with the anc.ML function of phytools and mapped onto the tree using the phytools function contMap.

2.6. Sequencing and phylogenetic analyses of plastid DNA regions

Since previously used plastid markers did not resolve relationships within *Luzula* (Záveská Drábková and Vlček, 2010), we identified two variable plastid regions (henceforth referred to as V1 and V5) based on plastome assemblies of nine species from *Luzula* sect. *Luzula* (Li et al., unpublished). We amplified and sequenced them for 159 individuals from 148 populations (Table S1). Amplification was performed for each region in a reaction mix (total volume 21 μl) containing 10.2 μl dH_2O, 7.73 μl REDTaq ReadyMix (Merck), 1.0 μl BSA (1 mg/μl; Promega), 0.53 μl of each primer (10 μM; LZ_V1_1_F and LZ_V1_1_R or LZ_V5_2_F and LZ_V5_1_R; Table S2) and 1 μl DNA template. PCR conditions for V1 were 5 min at 95 °C, 35 cycles of 30 s at 95 °C, 30 s at 61 °C and 2 min at 65 °C, followed by 10 min at 65 °C. The same conditions were used for V5, however with a lower annealing temperature of 57.2 °C. After purification of PCR products with *E. coli* Exonuclease I and SAP (Shrimp Alkaline Phosphatase; Fermentas) according to the manufacturer's instructions, Sanger sequencing was performed at Eurofins Genomics (Ebersberg, Germany) using the newly developed primers LZ_V1_1_F, LZ_V1_1_R and LZ_V1_S2_R for V1 and LZ_V5_2_F for V5 (Table S2). Contigs were assembled, aligned and edited in Geneious Pro v.5.5.9 (Kearse et al., 2012). Gaps (indels) were coded as binary characters using SeqState v.1.25 (Müller, 2005) applying simple gap coding (Simmons and Ochoterena, 2000).

A Bayesian phylogenetic tree was inferred from the concatenated plastid alignment using MrBayes v.3.2.7 (Ronquist et al., 2012) and applying the GTR (V1) and HKY + G (V5) substitution models proposed by the corrected Akaike information criterion (AICc) in MrAIC.pl v.1.4 (Nylander, 2004). The alignment was partitioned into nucleotide and indel sets, and indels were treated as morphological data (Lewis, 2001). The Metropolis-coupled Markov chain Monte Carlo process included four runs with four chains each (three heated using the default heating scheme) which were run simultaneously for 10,000,000 generations each. Trees were sampled every 1000th generation using default priors. PPs were determined from all trees whereas the first 1001 trees of each run were discarded as burn-in. Convergence of chains was assessed in Tracer v.1.7.2. Additionally, we constructed a ML tree with 1000 ultrafast bootstrap replicates in IQ-TREE 2, using the same substitution models as above with the JC2 model for binary indel data. Phylogeographic patterns were inferred from a statistical parsimony network built in TCS (Clement et al., 2000), implemented in POPART (Leigh and Bryant, 2015), applying a connection limit of 95 %.

3. Results

3.1. Phylogenetic relationships and temporal diversification within Luzula

The ML analysis of dataset 1 with 30 % minsl resulted in a well-resolved phylogenetic tree with high support values for the main clades (UBoot = 97–100; Fig. 2A). *Luzula* sect. *Luzula* was monophyletic and sister to *L. spicata* from *Luzula* sect. *Alpinae*. Sisters to them were *L. canariensis* and *L. sylvatica* from *Luzula* sect. *Anthelaea*. Sister to all of them was a clade formed by two lineages composed of (1) *L. forsteri*, *L. luzulina* and *L. pilosa* (all *Luzula* subgen. *Pterodes*), and (2) *L. alpinopilosa*, *L. glabrata* and *L. wahlenbergii* (all *Luzula* sect. *Diphrophyllatae*) intermixed with *L. luzuloides*, *L. lutea* and *L. nivea* (all *Luzula* sect. *Anthelaea*). Within *Luzula* sect. *Luzula*, *L. campestris* was sister to the remaining taxa, which were resolved into two main clades, one formed by *L. pallescens*, *L. africana*, *L. sudetica, L. abyssinica* and *L. stenophylla* (Clade A hereafter), and the other by *L. taurica*, *L. exspectata* and *L. divulgatiformis* (Clade B hereafter).

The topology of the chronogram, i.e. the dated species tree obtained with SNAPP (Fig. 2B), is mostly congruent with the ML tree, with the exception of *L. campestris* which was resolved as sister to Clade B of *Luzula* sect. *Luzula*, albeit with low support (PP = 0.7, Fig. 2B). The support values (PP) were between 0.8 and 1 in most branches; PP values below 0.5 were observed within Clade B. The stem age of *Luzula* sect. *Luzula* was dated to 3.95 millions of years ago (Ma) (95 % highest posterior densities, HPD: 3.21–4.73 Ma) in the mid-Pliocene, whereas the divergence between Clade A and Clade B plus *L. campestris* was estimated at 1.74 Ma (95 % HPD: 1.17–2.43 Ma; Fig. 2B). This was followed by the diversification of species within both clades starting in the mid-Pleistocene (Clade A: 1.62 Ma, 95 % HPD: 1.07–2.27 Ma; split of Clade B and *L. campestris*: 1.47 Ma, 95 % HPD: 0.93–2.13 Ma). Clade B diversified later than Clade A. The remaining *Luzula* species from other sections diverged between 1 and 5 Ma, from the early Pliocene to the mid-Pleistocene.

In the plastid tree (Fig. 3A), species of *Luzula* subgen. *Pterodes* formed the sister clade to all other taxa belonging to *Luzula* subgen. *Luzula*. Similarly to the tree based on the 3RADseq data (Fig. 2A), species of the sections *Anthelaea* and *Diphrophyllatae* were intermixed in a clade sister to all other members. Contrary to the ML tree inferred from the 3RADseq data where four accessions were included in the same clade, plastid sequences resolved two subsequently diverging clades of *Luzula* sect. *Anthelaea*, including (1) *L. sylvatica* 163 and *L. canariensis*, and (2) two accessions of *L. sylvatica*, respectively. Sister to them was a clade including *Luzula* sect. *Alpinae* and *L.* sect. *Luzula*. All these relationships were highly supported (PP 0.99 or 1; UBoot 91–100 %).

3.2. Phylogenetic relationships and genetic structure within Luzula sect. Luzula

The ML analysis focusing on *Luzula* sect. *Luzula* (dataset 2, 50 % minsl) resulted in a tree (Fig. 4A) where the phylogenetic relationships among *L. campestris* and Clades A and B were consistent with the genus phylogeny (dataset 1; Fig. 2A). Except for *L. taurica* and *L. divulgatiformis* that were paraphyletic, the species of *Luzula* sect. *Luzula* were recovered as monophyletic. Clade A included six main lineages forming two subclades. The first subclade included *L. abyssinica* nested within *L. sudetica*. The samples of *L. sudetica* from the Alps were sister to the single accession of *L. abyssinica* from eastern Africa and they together were sister to *L. sudetica* from the Balkan Peninsula, which we therefore treat as *L.* cf. *sudetica*. In the other subclade, *L. pallescens* and *L. africana* were sister species, and *L. stenophylla* was sister to them. In Clade B, different accessions of *L. taurica* formed a grade of basally divergent lineages, followed by a grade of paraphyletic *L. divulgatiformis* and monophyletic *L. exspectata* nested within. Within *L. taurica*, most early diverging

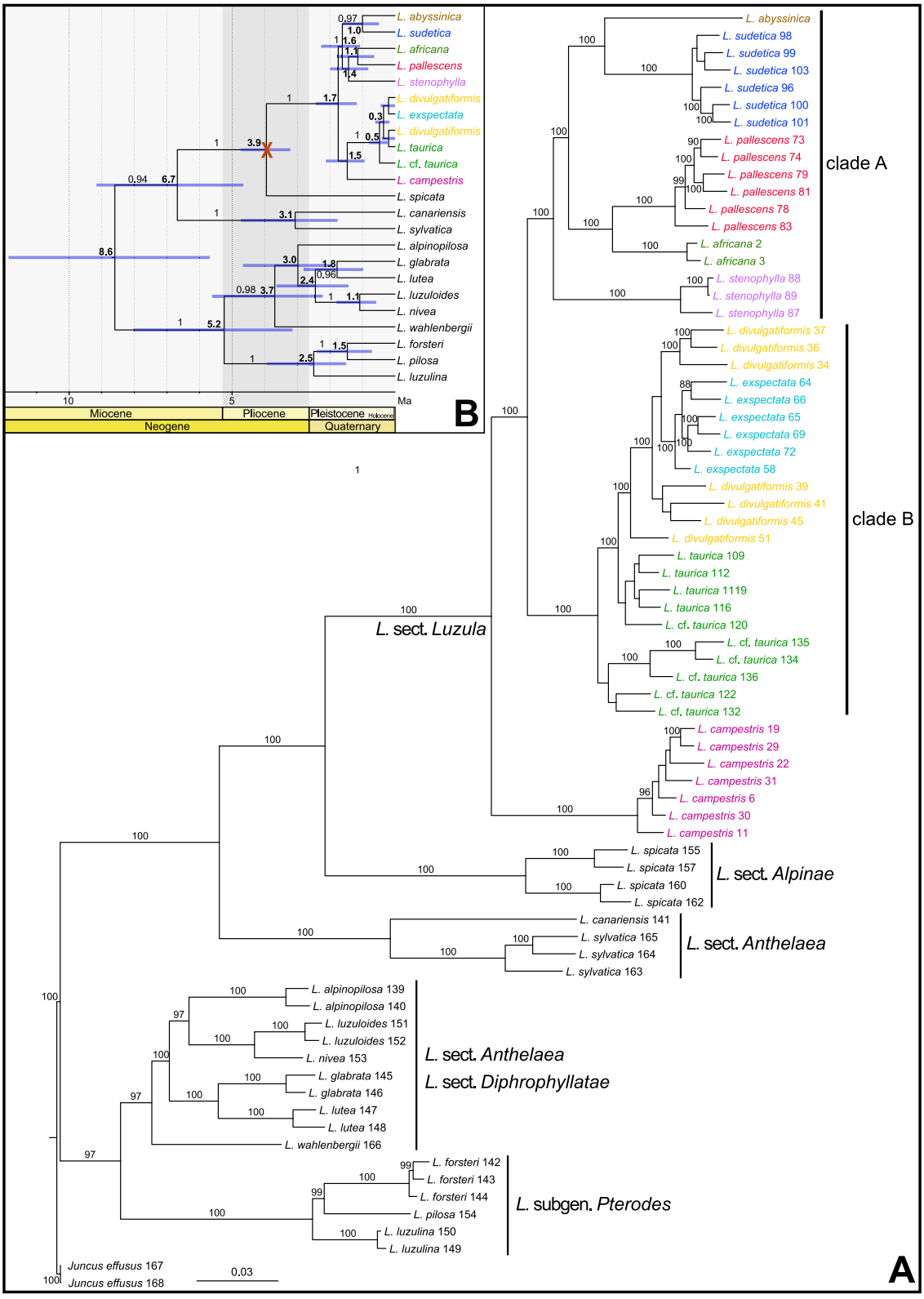

Fig. 2. Phylogenetic relationships and temporal diversification within *Luzula* based on 3RADseq data. (A) Best-scoring maximum likelihood tree based on 32,234 variable sites and inferred with IQ-TREE 2. Infrageneric taxa and two major clades of *Luzula* sect. *Luzula* are indicated. The numbers associated with branches are ultrafast bootstrap support values ≥ 95, the scale bar indicates the average number of substitutions per site, and the population IDs correspond to Table S1. (B) Divergence times estimates inferred with SNAPP based on 286 biallelic SNPs. Ages in millions of years from the present are indicated at nodes with numbers in bold and supplemented with bars representing the 95 % highest posterior densities. Numbers associated with branches are PP values > 0.9 The cross indicates the onset of diversification of *Luzula* sect. *Luzula*.

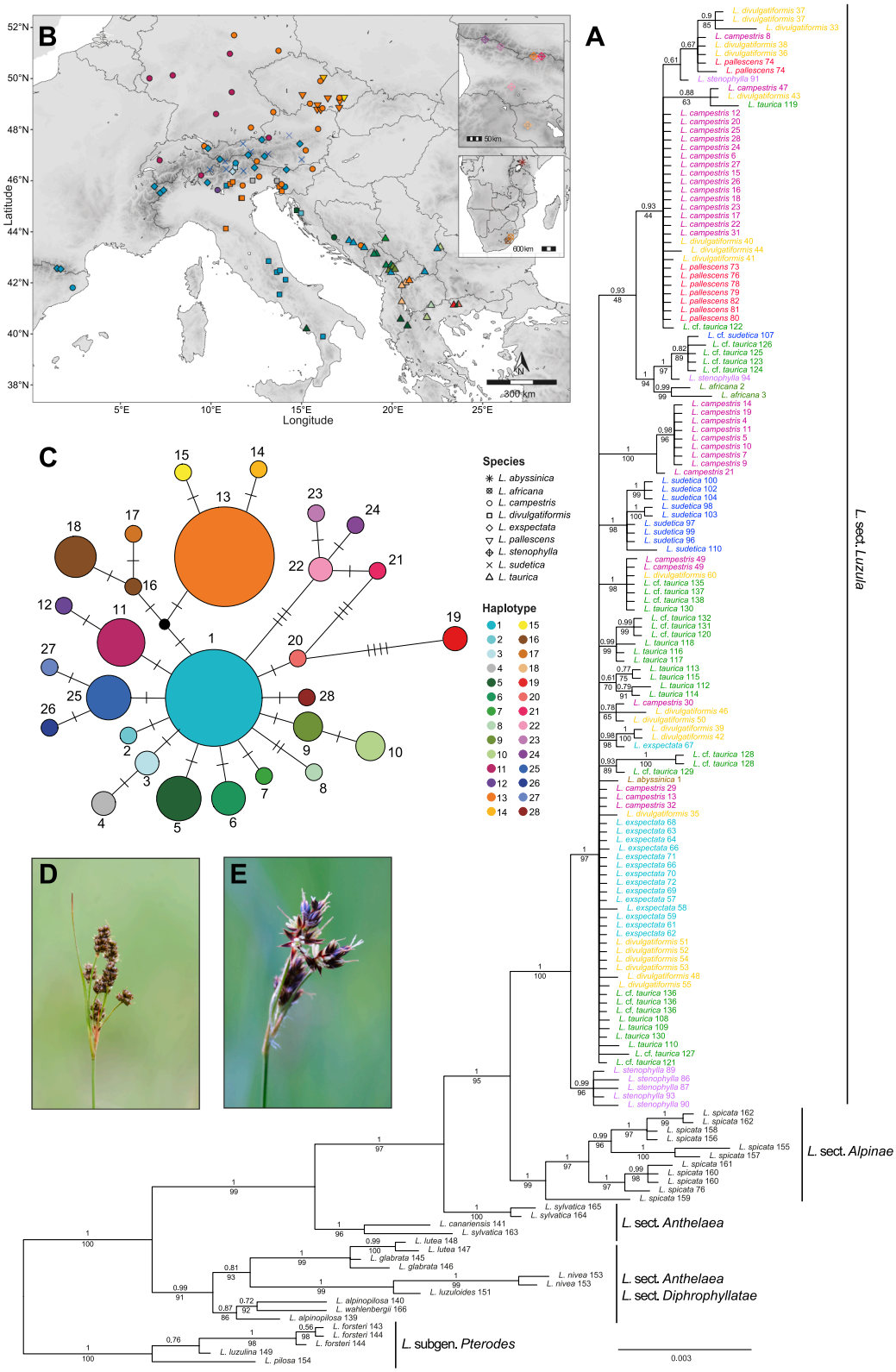

Fig. 3. Phylogenetic relationships within *Luzula* based on plastid DNA sequences. (A) Bayesian consensus phylogram inferred from concatenated plastid sequences in MrBayes. Numbers above branches are posterior probabilities and those below branches are ultrafast bootstrap support values inferred in IQ-TREE 2 for nodes that were recovered in both Bayesian and maximum likelihood analyses. Population IDs correspond to Table S1; infrageneric taxa are indicated. (B) Geographic distribution of plastid haplotypes. Species are represented by symbols and haplotypes are indicated by colours. (C) Statistical parsimony network of plastid haplotypes. Sizes of circles are proportional to the haplotypes' frequencies; colours and numbers are as in (B). Unsampled haplotypes are shown as black circles. (D) and (E) show typical inflorescences of *L. taurica* and *L. campestris*, respectively (Photos: V. Heimer).

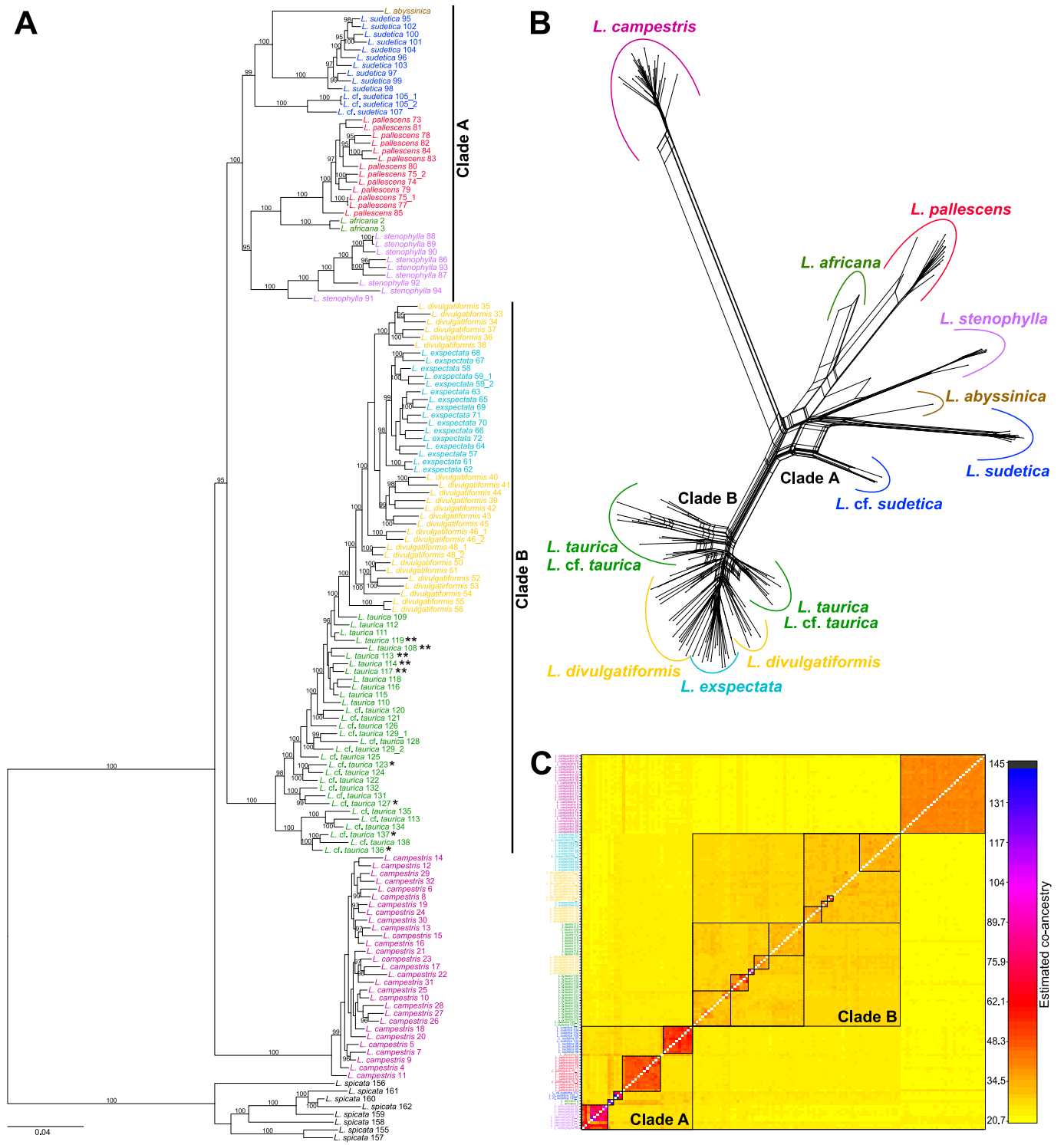

Fig. 4. Phylogenetic relationships and genetic structure within *Luzula* sect. *Luzula* based on 3RADseq data. (A) Best-scoring maximum likelihood tree inferred using IQ-TREE 2 based on 26,238 variable sites. The major clades within the section are indicated. Population IDs correspond to Table S1. Ultrafast bootstrap support values $\geq$ 95 are specified next to the branches. Asterisks indicate populations of *L. taurica* for which 24BL (one asterisk; *L.* cf. *taurica*) and 12AL (two asterisks) chromosomes were established. The scale bar indicates the average number of substitutions per site. (B) NeighborNet based on 2,701 biallelic SNPs. (C) Genetic structure inferred using fineRADstructure based on a coancestry matrix for pairs of individuals. The level of coancestry is colour-coded as indicated in the vertical bar on the right. The best-defined clusters are indicated.

lineages included samples with 24BL chromosomes and we therefore refer to these samples as *L.* cf. *taurica* (see section 2.1).

The three main lineages within *Luzula* sect. *Luzula*, corresponding to Clade A, Clade B, and *L. campestris*, were also recovered as distinct groups in the NeighborNet (Fig. 4B). The structure within Clades A and B largely corresponds to the ML tree (Fig. 4A), with clearer divergence among taxa in Clade A. Conversely, relationships within Clade B are less clear and shorter splits leading to them are consistent with their hypothesized younger age. These samples form loosely defined groups consistent with the ML topology, with both *L. taurica* (including *L.* cf.

taurica) and *L. divulgatiformis* being segregated into two clusters.

In the fineRADstructure analysis (Fig. 4C) the species from Clade A formed distinct groups, showing high coancestry values between conspecific samples, whereas the taxa of Clade B formed weakly defined clusters, with high coancestry among species. The substructure within Clade A shows five clearly defined clusters matching *L. africana*, *L. pallescens*, *L. sudetica*, *L.* cf. *sudetica* and *L. stenophylla,* plus the single *L. abyssinica* individual. *Luzula africana* and *L. pallescens* show some level of shared ancestry, while *L. abyssinica* displays shared ancestry with all other clusters of the clade except for *L. pallescens*. Despite high levels of coancestry among species in Clade B, several small clusters congruent with the groups recovered in the other analyses can be distinguished, and *L. taurica* was better delimited from *L.* cf. *taurica*. *Luzula campestris* formed a separated cluster, with coancestry signals shared only with a few samples of other species, particularly of Clade A.

The haplotype network of the plastid sequences of *Luzula* sect. *Luzula* resulted in 28 haplotypes that were mostly closely related and connected by one mutational step (Fig. 3C). There were two main haplotypes present in multiple samples across species. Haplotype 13 (orange) was found in *L. campestris, L. divulgatiformis, L. pallescens* and *L. taurica*, whereas haplotype 1 (turquoise) was present in *L. campestris, L. divulgatiformis, L. exspectata* and *L. taurica*. The species with the highest number (11) of haplotypes was *L. taurica*, where several different haplotypes were found in close proximity in the central and southern parts of the Balkan Peninsula. Within *L. campestris* there was a west (red) to east (orange) differentiation trend. The most divergent haplotypes 21, 22, 23 and 24 were found in *L. stenophylla* from the Caucasus, and in two individuals of *L.* cf. *taurica* from population 128 in north-eastern Greece (haplotype 19).

3.3. Genetic structure among *L. divulgatiformis, L. exspectata and L. taurica based on 3RADseq data*

The NeighborNet of Clade B of *Luzula* sect. *Luzula* (Fig. 5A) shows a structure with at least eight groups. All *L. exspectata* samples formed a single group on one side of the network, whereas the samples of *L. taurica* and *L.* cf. *taurica* fell in two groups. Samples of *L. divulgatiformis* were divided into five geographically separated groups from northern Italy, north-eastern Italy and Slovenia, Croatia, central Italy and southern Italy (Fig. 5A, C).

The analysis of genetic structure performed with tess3r inferred six groups (best-fit K = 6) within Clade B; all samples showed different proportions of admixture (Fig. 5B). With the exception of population 67, all samples of *L. exspectata* formed a cluster (violet) that extends across the northern margin of the distribution of Clade B, i.e., the Alps and the Pyrenees (Figs. 5B, C). The samples of *L. taurica* (including *L.* cf. *taurica*) were assigned to three groups: one (blue) in the central Balkans, another (red) in the south-eastern Balkans, and a third (orange), corresponding to *L.* cf. *taurica*, fragmented into four regions in the southwestern Balkans (Albania and Greece), the central Balkans (Bosnia and Herzegovina), the eastern Balkans (Serbia), and the southern Apennine (Italy). This last orange group is the one with the lowest signals of admixture (Fig. 5B). *Luzula divulgatiformis* was divided into two groups, one (pink) from northern Italy and westernmost Slovenia (including the divergent population 67 of *L. exspectata*), and the other (green) from the central and southern Apennine Peninsula and the Adriatic coast of the Balkan Peninsula (Croatia).

3.4. Chromosome numbers, genome size variation and its evolutionary dynamics

Chromosome counts revealed a 24BL cytotype for seven investigated populations (Table S1). All individuals had clearly more than 18 chromosomes, although the precise number of 24 could only be established for the samples 67 and 71. The samples 64, 67, 68 and 71 belonged to *L. exspectata* based on their morphology and phylogenetic position, whereas the samples 127, 136 and 137 were nested within *L. taurica* in phylogenetic analyses.

The smallest RGS was found in *L. pilosa* (0.172) whereas *L. alpinopilosa* (0.689) had the largest (Table S1, Fig. 6A). Among the

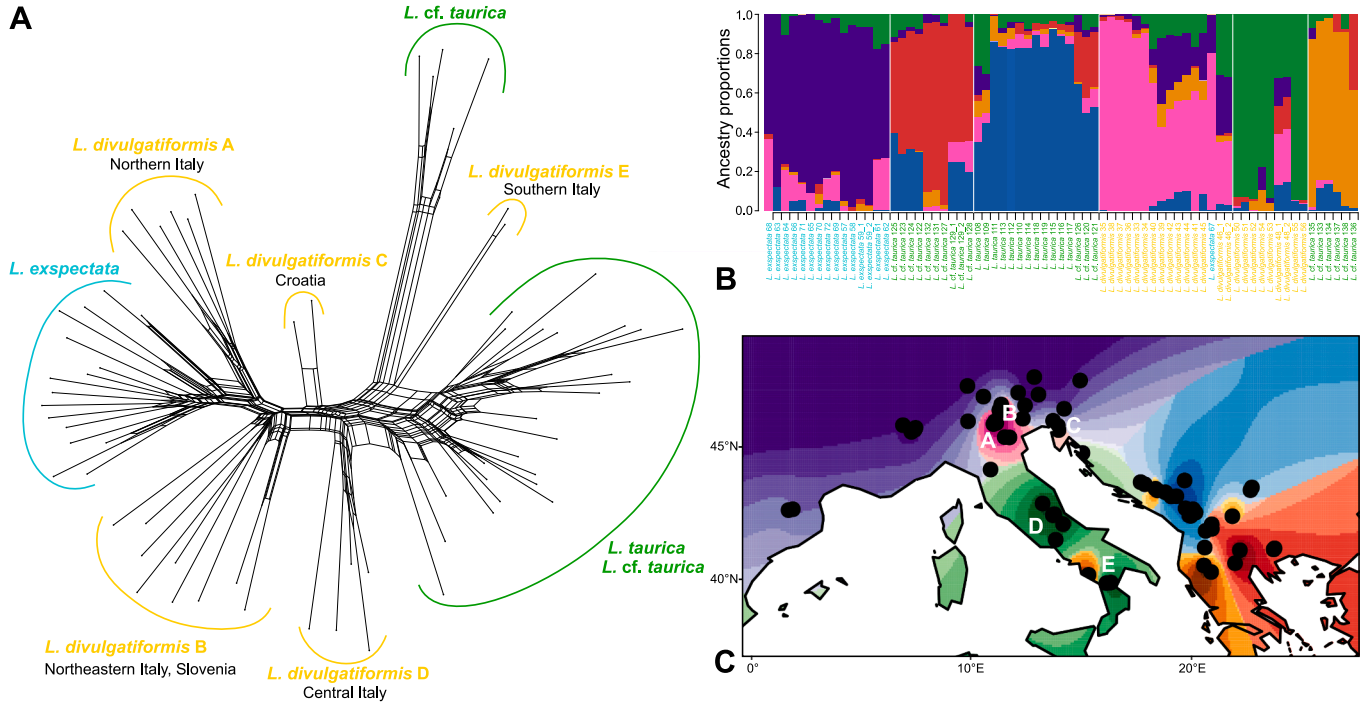

Fig. 5. Phylogenetic relationships and genetic structure among *Luzula divulgatiformis, L. exspectata* and *L. taurica* (Clade B of *Luzula* sect. *Luzula*) based on 3RADseq data. (A) NeighborNet based on 2,032 biallelic SNPs. (B) Genetic structure and (C) spatial interpolation of ancestry coefficients recovered at K = 6, inferred with tess3r based on 638 biallelic SNPs. The dots in C indicate sampling locations and the letters A–E correspond to the geographic regions identified for *L. divulgatiformis* in A.

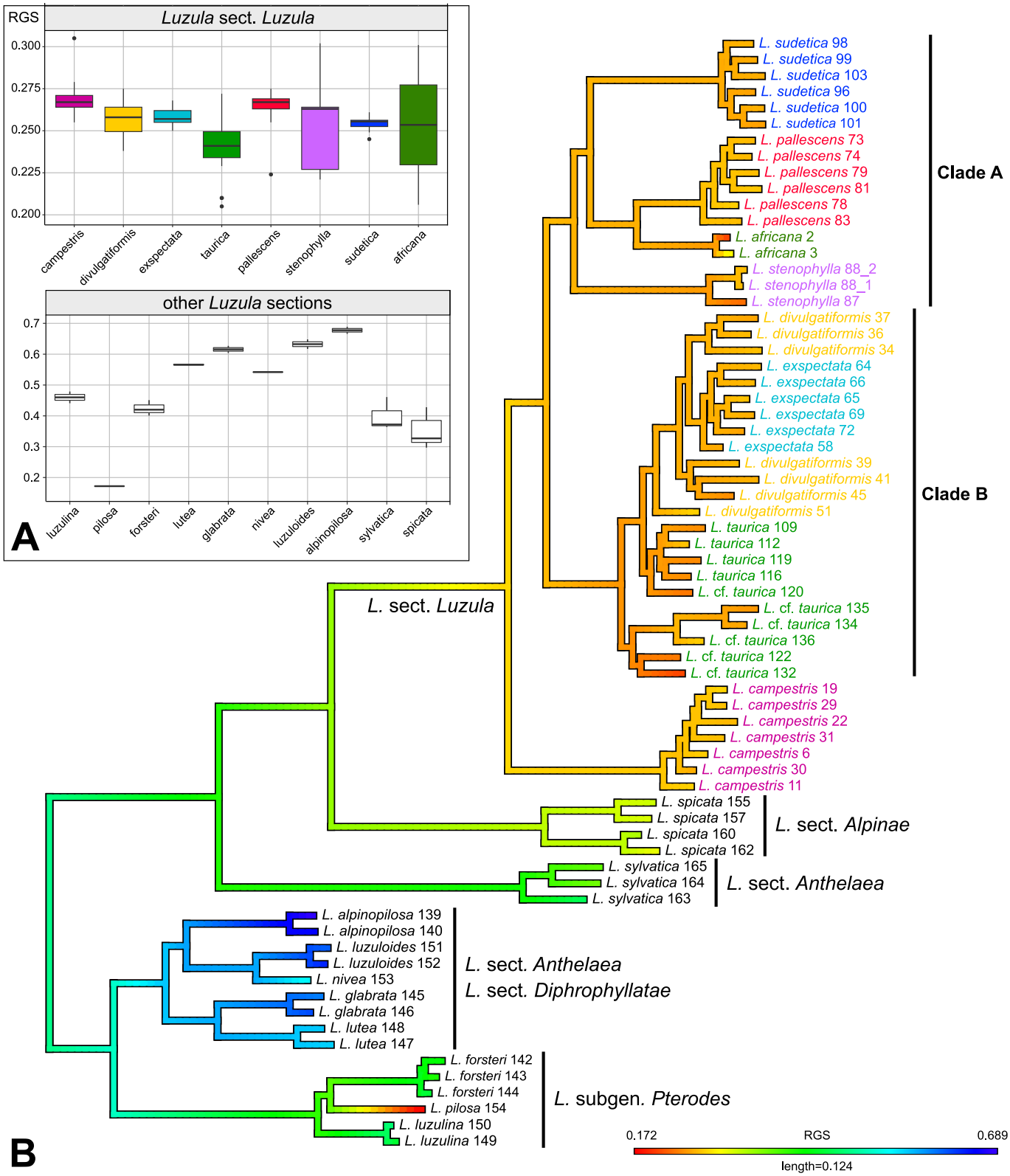

Fig. 6. (A) Variation of relative genome size (RGS) and (B) reconstruction of its evolution in *Luzula* inferred with phytools and indicated by colours corresponding to the colour ramp below the tree.

outgroup species, the RGS values recorded were 0.666–0.689 in *L. alpinopilosa*, 0.401–0.451 in *L. forsteri*, 0.604–0.627 in *L. glabrata*, 0.564–0.568 in *L. lutea*, 0.441–0.479 in *L. luzulina*, 0.617–0.648 in *L. luzuloides*, 0.542 in *L. nivea*, 0.172 in *L. pilosa*, 0.297–0.428 in *L. spicata*, and 0.364–0.461 in *L. sylvatica*. Within *Luzula* sect. *Luzula* the RGS varied between 0.205 (*L. taurica* 132) and 0.305 (*L. campestris* 5; Table S1, Fig. 6A). *Luzula africana* had an RGS of 0.206–0.301, *L. campestris* of 0.255–0.305, *L. divulgatiformis* of 0.238–0.275, *L. exspectata* of 0.250–0.268, *L. pallescens* of 0.224–0.275, *L. stenophylla* of 0.221–0.302, *L. sudetica* (incl. *L.* cf. *sudetica*) of 0.245–0.261, and

L. taurica (incl. *L.* cf. *taurica*) of 0.244–0.272.

There was a strong phylogenetic signal in the RGS as estimated with Pagel's λ (λ = 0.997, p < 0.0001). In accordance with the best-fitting EB model, substantial RGS changes are observed in the early evolution of *Luzula*, with a significant increase in RGS leading to the lineage including outgroup taxa such as *L. alpinopilosa* and *L. lutea*, and gradual downsizing in the lineage leading to *Luzula* sect. *Luzula*. In addition, a massive downsizing of RGS is observed in *L. pilosa* (Fig. 6B).

4. Discussion

The comprehensive phylogenomic approach applied here provides new insights into the evolutionary trends and diversification across diploid taxa of *Luzula* sect. *Luzula* distributed in the EAS and beyond, and their relationships to other major European groups of *Luzula*. Our results evidence that the patterns of genetic diversification differ between the two multi-species clades identified within *Luzula* sect. *Luzula* and indicate two putatively independent transitions towards agmatoploidy in these distinct lineages.

4.1. Phylogenetic relationships and temporal diversification within Luzula challenge traditional taxonomic concepts

Our phylogenetic reconstructions (Figs. 2, 3A) provide strong evidence for the monophyly of *Luzula* sect. *Luzula*. This is in line with previous studies relying on plastid sequencing analyses, where this section formed the only well-supported clade within *Luzula*, although with unresolved relationships to other sections (Záveská Drábková and Vlček, 2009). Our 3RADseq as well as plastid data clearly resolved *Luzula* sect. *Luzula* as one of the youngest lineages within the genus, sister to *Luzula* sect. *Alpinae* (*L. spicata*), with which it shares congested inflorescences (Kirschner, 2002). These two lineages diverged in the mid-Pliocene, with subsequent diversification of *Luzula* sect. *Luzula* in the Pleistocene (Fig. 2B). Similarly, while most of the major lineages within *Luzula* originated in the late Miocene or early Pliocene, most of the species evolved in the late Pliocene or Pleistocene, probably linked to the fragmentation of forests and expansion of grasslands due to gradual climatic cooling and drying (Suc and Zagwijn, 1983; Suc, 1984; Lisiecki and Raymo, 2005; Jiménez-Moreno et al., 2013).

Relationships inferred within *Luzula* strongly contrast traditional taxonomic concepts (Kirschner, 2002), despite the limited sampling. *Luzula sylvatica* and *L. canariensis* that were classified in *Luzula* sect. *Anthelaea*, are clearly divergent from *L. luzuloides*, *L. lutea* and *L. nivea* (Figs. 2, 3) that were also included in this section (Kirschner, 2002). The latter three species instead form a clade with *L. alpinopilosa*, *L. glabrata* and *L. wahlenbergii* from *Luzula* sect. *Diphrophyllatae*. In the ML tree based on 3RADseq data (Fig. 2) sisters to them are *L. forsteri, L. luzulina* and *L. pilosa* that were traditionally classified in *Luzula* subgen. *Pterodes* (Kirschner, 2002). On the other hand, these species are sister to all other taxa in the plastid tree (Fig. 3A). While *L. sylvatica* is monophyletic in the 3RADseq tree, it is resolved in two separated branches in the plastid tree, one of which also includes *L. canariensis*. Besides these two differences in topology between the 3RADseq and plastid trees, which can be a result of different inheritance modes, differential lineage sorting or hybridisation (Wendel and Doyle, 1998; Linder and Rieseberg, 2004; Okuyama et al., 2005; Frajman et al., 2009), the composition of the other main lineages and the relationships among them are congruent between both markers. Thus, our study indicates that the traditional classifications may not reflect the evolutionary history of the genus and thus calls for a revised taxonomic treatment, and also provides well-resolving plastid markers that can be used to infer general phylogenetic relationships among different groups of *Luzula*.

4.2. Evolution of agmatoploids and recent trans-continental diversification within Luzula sect. Luzula

The ML and SNAPP analyses produced highly congruent tree topologies, despite using disparate datasets, both in the number of samples and in the astringency applied to filter SNPs, reinforcing the reliability of the results for downstream evolutionary interpretations. Within *Luzula* sect. *Luzula*, several strongly supported clades at different levels of divergence can be distinguished. While molecular dating suggests that *Luzula* sect. *Luzula* originated in the late Pliocene 3.9 Ma, the diversification within this section was much delayed and had its onset in the (mid-)Pleistocene 1.7 Ma (Fig. 2B). *Luzula campestris*, a widespread diploid (2*n* = 12AL) species occurring mostly in lowlands up to the lower montane belt across Europe and North Africa, that is also morphologically distinct by having short underground stolons (Kirschner, 2002; Bačič et al., 2019), is sister to all other taxa in the ML-inferred trees (Figs. 2A, 4A). However, in the SNAPP-derived chronogram it is sister to Clade B (Fig. 2B), and in the NeighborNet it shares several parallel long splits with Clade A (Fig. 4B), indicating their shared ancestry. This incongruence may suggest reticulations early after the onset of diversification within *Luzula* sect. *Luzula* and/or incomplete lineage sorting. Genetic structure analysis shows coancestry signals between *L. campestris* and other species (Fig. 4C), whereas the plastid data reveal shared haplotypes with both *L. pallescens* from Clade A and *L. divulgatiformis* from Clade B (Fig. 3B).

Within Clade A, relationships at all levels are well-resolved (Figs. 2A, 4A) with little admixture between the clusters (Fig. 4C), which is consistent with the older age of this clade compared to Clade B, and thus an earlier onset of its diversification in the mid-Pleistocene, from 1.4 to 1.0 Ma (Fig. 2B). Similarly as in the case of *L. campestris*, there is an incongruence in the position of the Caucasian/north-east Anatolian *L. stenophylla* within Clade A. This species is resolved either as sister to all other taxa of Clade A in the phylogenetic trees, as sister to *L. africana* and *L. pallescens* (Figs. 2A, 4A), or as intermediate between the latter two species and *L. abyssinica* and *L. sudetica* in the NeighborNet (Fig. 4B). On the other hand, the sister-relationships between *L. africana* and *L. pallescens*, as well as between *L. abyssinica* and *L. sudetica*, are well supported, indicating very recent (Pleistocene) trans-continental dispersal events. Whereas *L. pallescens* is widely distributed in northern Eurasia, *L. africana* is endemic to southern Africa (Kirschner, 2002). Similarly, *L. sudetica* is widespread across European mountains, and *L. abyssinica* occurs in mountain grasslands of eastern tropical Africa (Kirschner, 2002). Our study indicates that the Balkan populations of *L. sudetica* (referred to as *L.* cf. *sudetica*) are clearly divergent from the Alpine populations and *L. abyssinica* is nested within them (Fig. 4A). Despite partial incongruences indicated by different types of analyses and thus relying on different number and composition of SNPs, *L. africana* and *L. abyssinica* are among the few evidenced recent dispersals between Europe and the African mountains. A few other studies have also shown that Plio-Pleistocene long distance dispersals from Eurasia prevail in the colonization of the sky islands in Africa (Hedberg, 1961; Gizaw et al., 2016; Brochmann et al., 2022). However, further studies with broader geographic sampling are needed to disentangle the relationships between *L. sudetica* and *L. abyssinica*.

In Clade A, different chromosome numbers and karyotypes have been reported, ranging from 12AL in *L. pallescens* (Nordenskiöld, 1951; Kirschner, 2002), over 12 (probably AL; Magulaev, 1992) to 24 (probably BL; Kirschner and Křisa, 1979) in *L. stenophylla* and 24BL in *L. abyssinica* (Nordenskiöld, 1951), to 48CL in *L. sudetica* (Nordenskiöld, 1951; Kirschner, 2002). There are no chromosome number reports for *L. africana*. Kirschner (1992) suggested that *L. sudetica* represents an agmatoploid derivative of *L. pallescens*, whereas Bačič et al. (2019) hypothesized that *L. exspectata* (24BL) might have been the parental species of *L. sudetica*. Our data clearly reject the latter hypothesis and show that *L. sudetica* is more closely related to *L. pallescens*, but shares even closer ancestry with *L. abyssinica*. It remains elusive whether *L. africana*

was involved in the origin of *L. sudetica*, which was accompanied by chromosome fragmentation and migration to Europe, or whether their common ancestor with 24BL chromosomes went extinct in Europe. *Luzula sudetica* is morphologically and ecologically distinct among the European members of *Luzula* sect. *Luzula* (Kirschner, 2002; Bačič et al., 2019) and it is therefore plausible that a more extensive sampling might uncover an evolutionary connection to an extra-European *Luzula* species.

4.3. Diversification of Luzula taurica and its allies within the European Alpine System

In contrast to Clade A, high levels of shared ancestry were found among the weakly resolved groups within Clade B (Fig. 4C), mirrored by short branches in the ML tree (Fig. 4A) as well as by the reticulation patterns in the NeighborNet (Fig. 5A). Diversification within Clade B, which is more recent than in Clade A, is estimated to have occurred within the last 0.5 Ma, which could explain the weak differentiation among species. Whereas *L. taurica* with 12AL chromosomes is widespread in Eurasia, from the Balkan Peninsula through the Pontic area and Anatolia to the Caucasus, the recently described *L. exspectata* and *L. divulgatiformis* (Bačič et al., 2007), both with 24BL chromosomes, have until now only been known from the Alps and southerly adjacent regions (Bačič et al., 2019). The circumscription of these three species is challenging in light of the present results, as both *L. taurica* and *L. divulgatiformis* are paraphyletic and form a grade of subsequently diverging lineages including monophyletic *L. exspectata* (Fig. 4A), this species sharing high levels of ancestry with *L. divulgatiformis* (Fig. 4C).

The earliest diverging lineage within Clade B is composed of individuals distributed in different parts of the Balkan Peninsula, along with one accession from the southern Apennine Peninsula (Fig. 4A). For two of these populations, 24BL chromosomes have been established (Fig. 4A, Table S1; Bačič et al., 2016) and we refer to this clade as *L.* cf. *taurica*. Although these populations could potentially belong to *L. fallax*, a species from the southern Balkan Peninsula (from Albania to Bulgaria and European Turkey), but with unknown exact distribution (Kirschner, 2002), we found no morphological indications for that. In any case, the Italian population nested within the Balkan accessions is an example of a recent trans-Adriatic dispersal (Frajman and Schönswetter, 2017), likely from the Balkan to the Apennine Peninsula.

The remaining samples of *L. taurica* (including *L.* cf. *taurica* based on two available chromosome counts) that diverge successively in the ML tree (Fig. 4A), form a rather clear, although genetically diverse, cluster in the NeighborNet (Fig. 5A). However, they are assigned to two groups in the genetic structure analysis, and are geographically differentiated in north-west to south-east direction in the Balkan Peninsula (Fig. 5B, C). This, along with the high plastid haplotype diversity (Fig. 3B, C), is consistent with the well-known higher genetic diversity in the central and southern Balkan Peninsula compared to northerly adjacent areas in many plant groups (Đurović et al., 2021; Španiel and Rešetnik, 2022).

Similarly to *L. taurica*, *L. divulgatiformis* forms a grade of subsequently diverging lineages in the ML tree, although mostly with better support for the lineages compared to *L. taurica* (Fig. 4A). These lineages are nested within *L. taurica*, which is consistent with the hypothesis that the latter species was involved in the agmatoploid origin of *L. divulgatiformis* (Bačič et al., 2007), but also questions the taxonomic delimitation between both taxa. Specifically, some populations from the Balkan Peninsula that are morphologically similar to *L. taurica* had 24BL chromosomes (Bačič et al., 2016), which is the karyotype characteristic for *L. divulgatiformis* (Bačič et al., 2007, 2019). Also in the NeighborNet there are several clearly differentiated clusters of *L. divulgatiformis* including geographically proximate populations (Fig. 5A). In contrast, the genetic structure inferred with tess3r assigned the samples of *L. divulgatiformis* to only two genetic groups with high levels of admixture with other groups (Fig. 5B). These two groups are geographically correlated. The southern (green) group has an amphi-Adriatic distribution, extending across most of the Apennine Peninsula with a disjunction in the north-western Balkan Peninsula. This provides new evidence that *L. divulgatiformis* is much more widely distributed than previously assumed (Bačič et al., 2016, 2019), but also questions its delimitation not only from *L. taurica*, but also from *L. calabra*, a species with 24BL chromosomes that is considered endemic to the southern Apennine Peninsula (Kirschner, 2002). The northern genetic cluster of *L. divulgatiformis* (pink) extends along the southern margin of the Eastern Alps, from where the species was described (Bačič et al., 2007). This cluster also included population 67 of *L. exspectata* from Northern Italy (Fig. 5B).

Finally, *L. exspectata* is monophyletic and nested within the northern populations of *L. divulgatiformis*, from which it likely originated. Given the young age of divergence between both species (0.2 Ma, Fig. 2B), we hypothesize that the origin of this lineage was connected to adaptation to alpine habitats during one of the last glacial cycles, when climatic conditions also enabled westward migration to the Pyrenees. Recent colonization of the Pyrenees from the Alps was inferred also in other plant groups inhabiting alpine habitats (e.g., Schönswetter et al., 2002; Frajman and Oxelman, 2007; Đurović et al., 2017). Our data, thus, indicate for the first time the presence of *L. exspectata* outside the Alps and also provide additional information about its presence in the Western Alps (see Bačič et al., 2019).

In summary, there is a strong geographic component in the distribution of genetic diversity within Clade B, which only partially conforms to currently recognized species boundaries and rather shows a gradual south-to-north transition from *L. taurica* over *L. divulgatiformis* to *L. exspectata*, which should probably be better treated as subspecies.

In light of the recent origin of Clade B, we hypothesize that common ancestry associated with low differentiation, i.e., ongoing speciation, are the main causes for the observed phylogenetic pattern. Alternatively, differential and incomplete lineage sorting, along with more recent hybridisations and occasional gene flow between diverging lineages, could have contributed to the observed genetic admixture and paraphyly. To better understand these processes, population-level analyses focusing on fine-scale genetic structure and gene flow would likely be necessary to accurately assess the extent of hybridisation and introgression within this clade. The minor morphological differences between *L. divulgatiformis* and *L. exspectata* (Bačič et al., 2007, 2019) are likely a result of adaptation to lowland submediterranean vs. alpine habitats, respectively. In addition, karyotype differentiation between 12AL and 24BL that took place at least once within this clade, partly contributes to the divergence of some of the lineages (e.g., the lineage with several individuals having 12AL chromosomes is well-supported), but also trans-Adriatic migrations that occurred at least twice within this clade certainly resulted in genetic isolation of populations on both sides of the Adriatic Sea. Finally, our study clearly demonstrates the need for further studies focusing on the Apennine and Balkan peninsulas, applying phylogenetic, cytogenetic and morphometric methods to a geographically dense sampling.

4.4. Insights into the origin(s) of agmatoploidy and genome size evolution in Luzula

It has been suggested that the transition to holocentricity in the grass order Poales occurred more than 60 Ma, given its presence in both Cyperaceae and Juncaceae (Hofstatter et al., 2022). Although *Juncus* was recently identified as a genus with monocentric chromosomes (Mata-Sucre et al., 2023), dynamic centromeres have been found in *J. effusus* and may represent a transient state between mono- and holocentricity (Dias et al., 2024). Holocentricity is thus likely an ancestral state that would have influenced the diversification within *Luzula* by enabling karyotypic changes via agmatoploidy and symploidy. The ancestor of agmatoploid species in *Luzula* has been hypothesized to be a diploid with full-size chromosomes (Kirschner, 1992; Bačič et al., 2019; Pungaršek et al., 2023), but it is not clear whether such diploid ancestors

are still extant today. Given that (1) *L. sylvatica* and *L. spicata*, which are sister to *Luzula* sect. *Luzula*, include diploid populations with 12AL chromosomes (Nordenskiöld 1951), (2) *L. campestris*, which also has 12AL chromosomes, is likely sister to Clades A and B, and (3) Clades A and B include *L. pallescens* and *L. taurica,* both with 12AL chromosomes, it can be hypothesized that the species with 24BL and 48CL chromosomes are derived within *Luzula* sect. *Luzula*. We inferred at least two fragmentation events in Clade A, leading to the 24BL chromosomes of *L. abyssinica* and the 48CL chromosomes of *L. sudetica.* However, it is possible that an additional chromosome fragmentation occurred in the lineage of *L. stenophylla*. On the other hand, 24BL chromosomes possibly had multiple origins within Clade B, given their scattered occurrences across the clade. The presence of agmatoploids in other lineages of *Luzula* (e.g., in some populations of *L. spicata* or in *L. wahlenbergii*; Nordenskiöld, 1951, Kirschner, 2002), indicates multiple transitions towards agmatoploidy within the genus. Nevertheless, a thorough reconstruction of karyotypes will be necessary in order to unveil the exact dynamics of agmatoploidisation within *Luzula*.

Holocentric chromosomes, like those in *Luzula* species, have adaptations in cell division that may promote rapid karyotype evolution by facilitating the fixation of new chromosome arrangements (Steckenborn and Marques, 2025). In *Carex*, another genus with holocentric chromosomes from the sister family Cyperaceae, chromosomal rearrangements such as fusion and fission have been reported to play a crucial role in genetic differentiation and speciation (Escudero et al., 2010; Hipp et al., 2010; Tribble et al., 2024), but were also crucial for adaptation to changing environments (Escudero et al., 2012). Recombination as a fundamental evolutionary process generating genetic diversity and strongly affecting evolutionary processes has been shown to be strongly affected by karyotype differences; recombination rates thus increase with chromosome number and decrease with mean chromosome size (Näsvall et al., 2023; Zedek et al., 2025). Holocentric chromosomes tolerate fragmentation from clastogenic agents such as UV radiation or desiccation, which is a key adaptive advantage (Zedek and Bureš, 2018). Although holocentric lineages generally diversify more slowly than monocentric ones (Zedek and Bureš, 2018), their karyotypic rearrangements are powerful drivers of species diversification, especially under severe environmental pressures (Steckenborn and Marques, 2025). In *Luzula* sect. *Luzula*, concerted chromosome fragmentations could then emerge as an important promoter of genetic variability, driving diversification in the section (e.g., genetic groups resolved among the species of clade B). This might have been connected to the colonization of open alpine habitats with increased UV radiation, which can trigger chromosomal fissions (Zedek and Bureš, 2018), thus leading to increased recombination rates compared to the ancestral populations (Zedek et al., 2025). This is particularly valuable in organisms with holocentric chromosomes, where only one or at most two crossovers have been evidenced per chromosome (Zedek et al., 2025).

In addition to changes in chromosome numbers, our reconstruction of evolutionary dynamics in genome size across *Luzula* (Fig. 6B) indicates both up- and downsizing trends. Genome upsizing happened in the lineage leading to *L. alpinopilosa*, *L. lutea* and related species, all of which have 12AL chromosomes, except for *L. wahlenbergii* which has 24BL chromosomes (Nordenskiöld, 1951; Kirschner, 2002). In contrast, gradual genome downsizing happened in the lineage including *L. spicata* and *Luzula* sect. *Luzula*, but in particular in the evolution of the latter section. This tendency to smaller genomes in *Luzula* sect. *Luzula* compared with the rest of the genus was previously hypothesized by superimposing chromosome numbers and genome size measurements on a phylogenetic tree (Bozek et al., 2012). Our study also indicates a drastic decrease in genome size of *L. pilosa*, compared to closely related *L. forsteri* and *L. luzulina*. Whereas the last two species both have 24BL chromosomes, a high number (66–72) of very small chromosomes smaller than the CL-type have been registered for *L. pilosa*, in which chromosome fragmentations were apparently associated with genome downsizing. This is not the case in *Luzula* sect. *Luzula*, where agmatoploidy was not accompanied by substantial changes in genome size, as previously reported (Bačič et al., 2019).

In summary, both chromosomal fissions as well as genome down- and upsizings, resulting in 4-fold differences in genome size among diploid species of *Luzula*, have contributed to diversification within this genus with intricate evolutionary history. Although our study resolved some long-standing questions, many still remain to be answered. In addition, adding true polyploids to the analyses will certainly add another level of complexity. Hedda Nordenskiöld (1951) who pioneered the cytogenetic studies in *Luzula* started her paper with the sentence "This study has been made as an orientation in the taxonomical problems of the genus *Luzula* in relation to its cytology with the object of using the results as a basis for further cyto-taxonomical investigations". Along the same line, our study will hopefully serve as an orientation for future phylogenetic studies of *Luzula*, gradually shedding more light on processes driving diversification of these inconspicuous but highly intriguing organisms.

CRediT authorship contribution statement

Carolina Carrizo García: Writing – review & editing, Writing – original draft, Visualization, Methodology, Investigation, Formal analysis, Data curation, Conceptualization. **Valentin Heimer:** Writing – review & editing, Writing – original draft, Visualization, Resources, Methodology, Investigation, Formal analysis, Data curation. **Peter Schönswetter:** Writing – review & editing, Conceptualization. **Claudio Varotto:** Writing – review & editing, Supervision, Investigation, Conceptualization. **Božo Frajman:** Writing – review & editing, Writing – original draft, Visualization, Validation, Supervision, Project administration, Methodology, Investigation, Funding acquisition, Formal analysis, Conceptualization. **Mingai Li:** Writing – review & editing, Supervision, Project administration, Methodology, Investigation, Funding acquisition, Conceptualization.

Funding

This research was funded by the European Region Tyrol-South Tyrol-Trentino (EGTC) through the Euregio Science Fund, project LUZALP – IPN 133, 4th call 2020.

Declaration of competing interest

The authors declare that they have no known competing financial interests or personal relationships that could have appeared to influence the work reported in this paper.

Acknowledgements

We thank T. Elliot for providing the chronogram of Poales and F. Zedek for providing some samples. We also thank L. Angelini, T. Bačič, L. Baldaszti, G. Bartolomeo, D. Baumgartner, S. Bogdanović, P. Bureš, J. Czogalla, D. Dietrich, M. Doboš, J. Dolenc Koce, A. Hilpold, N. Kremml, F. Faltner, J. Geurden, A. Háková, M. Heck, W. Heimer, I. Heimer, A. Heimer, J. Heimer, M. Helling, S. Kleiner, D. Kutnjak, Ž. Lobnik Cimerman, M. Magauer, J. Maindok, V. Margreiter, A. Mayerova, E. Nitz, D. Pirkebner, J. Plunger, Š. Pungaršek, I. Pungaršek, N. Rainer, L. Reiterová, U. Schmidt, L. Silbernagl, G. Span, N. Steixner, V. Stojilkovič, P. Šmarda, F. Tilg, A. Wylie and T. Zeni for help during field and/or laboratory work and T. Bačič for inspiring discussions about *Luzula*.

Appendix A. Supplementary data

Supplementary data to this article can be found online at https://doi.org/10.1016/j.ympev.2025.108455.

Data availability

Raw sequence reads used in this study are publicly available at NCBI under the BioProject PRJNA1225458. GenBank numbers of plastid sequences are in Table S1.

References

Aeschimann, D., Lauber, K., Moser, D.M., Theurillat, J.-P., 2004. Flora Alpina. Zanichelli, Berlin.

Andrews, S., 2010. FastQC: A quality control tool for high throughput sequence data. https://www.bioinformatics.babraham.ac.uk/projects/fastqc/ (accessed 7 January 2025).

Arante Chaves, A.L., Ferreira, M.T.M., Escudero, M., Luceño, M., Costa, S.M., 2024. Chromosomal evolution in Cryptangieae Benth. (Cyperaceae): evidence of holocentrism and pseudomonads. Protoplasma 261, 527–541. https://doi.org/10.1007/s00709-023-01915-w.

Bačič, T., Dolenc Koce, J., Frajman, B., 2019. Diversification and distribution patterns of *Luzula* sect. *Luzula* (Juncaceae) in the Eastern Alps: a cytogenetic approach combined with extensive herbarium revisions. Alpine Bot. 129, 149–161. https://doi.org/10.1007/s00035-019-00219-1.

Bačič, T., Frajman, B., Dolenc Koce, J., 2016. Diversification of *Luzula* sect. *Luzula* (Juncaceae) on the Balkan Peninsula – a cytogenetic approach. Folia Geobot. 51, 51–63. https://doi.org/10.1007/s12224-016-9235-2.

Bačič, T., Jogan, N., Dolenc Koce, J., 2007. *Luzula* sect. *Luzula* in the south-eastern Alps—karyology and genome size. Taxon 56, 129–136. https://doi.org/10.2307/25065743.

Bayona-Vásquez, N.J., Glenn, T.C., Kieran, T.J., Pierson, T.W., Hoffberg, S.L., Scott, P.A., Bentley, K.E., Finger, J.W., Louha, S., Troendle, N., Diaz-Jaimes, P., Mauricio, R., Faircloth, B.C., 2019. Adapterama III: Quadruple-indexed, double/triple-enzyme RADseq libraries (2RAD/3RAD). PeerJ, e7724. https://doi.org/10.7717/peerj.7724.

Bouckaert, R., Vaughan, T.G., Barido-Sottani, J., Duchêne, S., Fourment, M., Gavryushkina, A., Heled, J., Jones, G., Kühnert, D., De Maio, N., Matschiner, M., Mendes, F.K., Müller, N.F., Ogilvie, H.A., du Plessis, L., Popinga, A., Rambaut, A., Rasmussen, D., Siveroni, I., Suchard, M.A., Wu, C.-H., Xie, D., Zhang, Ch., Stadler, T., Drummond, A.J., 2019. BEAST 2.5: an advanced software platform for Bayesian evolutionary analysis. PLoS Comput. Biol. 15, e1006650. https://doi.org/10.1371/journal.pcbi.1006650.

Bozek, M., Leitch, A.R., Leitch, I.J., Záveská Drábková, L., Kuta, E., 2012. Chromosome and genome size variation in *Luzula* (Juncaceae), a genus with holocentric chromosomes. Bot. J. Linn. Soc. 170, 529–541. https://doi.org/10.1111/j.1095-8339.2012.01314.x.

Brochmann, C., Gizaw, A., Chala, D., Kandziora, M., Eilu, G., Popp, M., Pirie, M.D., Gehrke, B., 2022. History and evolution of the afroalpine flora: in the footsteps of Olov Hedberg. Alp. Botany 132, 65–87. https://doi.org/10.1007/s00035-021-00256-9.

Brožová, V., Proćków, J., Záveská Drábková, L., 2022. Toward finally unraveling the phylogenetic relationships of Juncaceae with respect to another cyperid family. Cyperaceae. Mol. Phylogenet. Evol. 177, 107588. https://doi.org/10.1016/j.ympev.2022.107588.

Bryant, D., Bouckaert, R., Felsenstein, J., Rosenberg, N.A., RoyChoudhury, A., 2012. Inferring species trees directly from biallelic genetic markers: bypassing gene trees in a full coalescent analysis. Mol. Biol. Evol. 29, 1917–1932. https://doi.org/10.1093/molbev/mss086.

Bureš, P., Zedek, F., Marková, M., 2013. Holocentric chromosomes. In: Wendel, J., Greilhuber, J., Doležel, J., Leitch, I.J. (Eds.), Plant genome diversity volume 2: physical structure, behaviour and evolution of plant genomes. Springer, Heidelberg, pp. 187–208. https://doi.org/10.1007/978-3-7091-1160-4_12.

Catchen, J., Hohenlohe, P., Bassham, S., Amores, A., Cresko, W., 2013. Stacks: an analysis tool set for population genomics. Mol. Ecol. 22, 3124–3140. https://doi.org/10.1111/mec.12354.

Caye, K., Deist, T., Martins, H., Michel, O., Francois, O., 2016. TESS3: fast inference of spatial population structure and genome scans for selection. Mol. Ecol. Res. 16, 540–548. https://doi.org/10.1111/1755-0998.12471.

Clement, M., Posada, D., Crandall, K.A., 2000. TCS: a computer program to estimate gene genealogies. Mol. Ecol. 9, 1657–1659.

Danecek, P., Auton, A., Abecasis, G., Albers, C.A., Banks, E., DePristo, M.A., Handsaker, R., Lunter, G., Marth, G., Sherry, S.T., McVean, G., Durbin, R., 1000 Genomes Project Analysis Group, 2011. The variant call format and VCFtools. Bioinformatics 27, 2156–2158. https://doi.org/10.1093/bioinformatics/btr330.

Dias, Y., Mata-Sucre, Y., Thangavel, G., Costa, L., Báez, M., Houben, A., Marques, A., Pedrosa-Harand, A., 2024. How diverse a monocentric chromosome can be? Repeatome and centromeric organization of *Juncus effusus* (Juncaceae). Plant J. 118, 1832–1847. https://doi.org/10.1111/tpj.16712.

Drábková, L., Kirschner, J., Seberg, O., Petersen, G., Vlček, Č., 2003. Phylogeny of the Juncaceae based on *rbc*L sequences, with special emphasis on *Luzula* DC. and *Juncus* L. Plant Syst. Evol. 240, 133–147. https://doi.org/10.1007/s00606-003-0001-6.

Drábková, L., Kirschner, J., Vlček, Č., 2006. Phylogenetic relationships within *Luzula* DC. and *Juncus* L. (Juncaceae): a comparison of phylogenetic signals of *trn*L-*trn*F intergenic spacer, *trn*L intron and *rbc*L plastome sequence data. Cladistics 22, 132–143. https://doi.org/10.1111/j.1096-0031.2006.00095.x.

Đurović, S., Schönswetter, P., Niketić, M., Tomović, G., Frajman, B., 2017. Disentangling relationships among the members of the *Silene saxifraga* alliance (Caryophyllaceae): phylogenetic structure is geographically rather than taxonomically segregated. Taxon 66, 343–364. https://doi.org/10.12705/662.4.

Đurović, S.Z., Temunović, M., Niketić, M., Tomović, G., Schönswetter, P., Frajman, B., 2021. Impact of Quaternary climatic oscillations on phylogeographic patterns of three habitat-segregated *Cerastium* taxa endemic to the Dinaric Alps. J. Biogeogr. 48, 2022–2036. https://doi.org/10.1111/jbi.14133.

Eaton, D.A.R., Overcast, I., 2020. ipyrad: Interactive assembly and analysis of RADseq datasets. Bioinformatics 36, 2592–2594. https://doi.org/10.1093/bioinformatics/btz966.

Edgar, E., 1966. *Luzula* in New Zealand. New Zeal. J. Bot. 4, 159–184.

Elliott, T.L., Spalink, D., Larridon, I., Zuntini, A.R., Escudero, M., Hackel, J., Barrett, R.L., Martín-Bravo, S., Márquez-Corro, J.I., Granados Mendoza, C., Mashau, A.C., Romero-Soler, K.J., Zhigila, D.A., Gehrke, B., Andrino, C.O., Crayn, D.M., Vorontsova, M.S., Forest, F., Baker, W.J., Wilson, K.L., Simpson, D.A., Muasya, A.M., 2024. Global analysis of Poales diversification – parallel evolution in space and time into open and closed habitats. New Phytol. 242, 727–743. https://doi.org/10.1111/nph.19421.

Escudero, M., Balao, F., Martín-Bravo, S., Valente, L., Valcárcel, V., 2018. Is the diversification of Mediterranean Basin plant lineages coupled to karyotypic changes? Plant Biol. J 20, 166–175. https://doi.org/10.1111/plb.12563.

Escudero, M., Hipp, A.L., Luceño, M., 2010. Karyotype stability and predictors of chromosome number variation in sedges: a study in *Carex* section *Spirostachyae* (Cyperaceae). Mol. Phylogenet. Evol. 57, 353–363. https://doi.org/10.1016/j.ympev.2010.07.009.

Escudero, M., Hipp, A.L., Waterway, M.J., Valente, L.M., 2012. Diversification rates and chromosome evolution in the most diverse angiosperm genus of the temperate zone (*Carex*, Cyperaceae). Mol. Phylogenet. Evol. 63, 650–655. https://doi.org/10.1016/j.ympev.2012.02.005.

Escudero, M., Márquez-Corro, J.I., Hipp, A., 2016. The phylogenetic origins and evolutionary history of holocentric chromosomes. Syst. Bot. 41, 580–585. https://doi.org/10.1600/036364416X692442.

Frajman, B., Eggens, F., Oxelman, B., 2009. Hybrid origins and homoploid reticulate evolution within *Heliosperma* (Sileneae, Caryophyllaceae) – a multigene phylogenetic approach with relative dating. Syst. Biol. 58, 328–345. https://doi.org/10.1093/sysbio/syp030.

Frajman, B., Oxelman, B., 2007. Reticulate phylogenetics and phytogeographical structure of *Heliosperma* (Sileneae, Caryophyllaceae) inferred from chloroplast and nuclear DNA sequences. Mol. Phylogenet. Evol. 43, 140–155. https://doi.org/10.1016/j.ympev.2006.11.003.

Frajman, B., Schönswetter, P., 2017. Amphi-Adriatic distributions in plants revisited: Pleistocene trans-Adriatic dispersal in the *Euphorbia barrelieri* group (Euphorbiaceae). Bot. J. Linn. Soc. 185, 240–252. https://doi.org/10.1093/botlinnean/box055.

Gizaw, A., Brochmann, C., Nemomissa, S., Wondimu, T., Masao, C.A., Tusiime, F.M., Abdi, A.A., Oxelman, B., Popp, M., Dimitrov, D., 2016. Colonization and diversification in the African "sky islands": insights from fossil-calibrated molecular dating of *Lychnis* (Caryophyllaceae). New Phytol 211, 719–734. https://doi.org/10.1111/nph.13937.

Guerra, M., 2016. Agmatoploidy and symploidy: a critical review. Genet. Mol. Biol. 39, 492–496. https://doi.org/10.1590/1678-4685-GMB-2016-0103.

Hedberg, O., 1961. The phytogeographical position of the afroalpine flora. Rec. Adv. Bot. 1, 914–919.

Hipp, A.L., Rothrock, P.E., Whitkus, R., Weber, J.A., 2010. Chromosomes tell half of the story: the correlation between karyotype rearrangements and genetic diversity in sedges, a group with holocentric chromosomes. Mol. Ecol. 19, 3124–3138. https://doi.org/10.1111/j.1365-294X.2010.04741.x.

Hoang, D.T., Chernomor, O., von Haeseler, A., Minh, B.Q., Vinh, L.S., 2018. UFBoot2: improving the ultrafast bootstrap approximation. Mol. Biol. Evol. 35, 518–522. https://doi.org/10.1093/molbev/msx281.

Hofstatter, P.G., Thangavel, G., Lux, T., Neumann, P., Vondrak, T., Novak, P., Zhang, M., Costa, L., Castellani, M., Scott, A., Toegelová, H., Fuchs, J., Mata-Sucre, Y., Dias, Y., Vanzela, A.L.L., Huettel, B., Almeida, C.S.S., Šimková, H., Souza, G., Pedrosa-Harand, A., Macas, J., Mayer, K.F.X., Houben, A., Marques, A., 2022. Repeat-based holocentromeres influence genome architecture and karyotype evolution. Cell 185, 3153–3168. https://doi.org/10.1016/j.cell.2022.06.045.

Hultén, M.A., 2013. Kinetochore. In: Brenner's Encyclopedia of Genetics, second Edition. Academic Press, London, pp. 168–169. https://doi.org/10.1016/B978-0-12-374984-0.00834-2.

Huson, D.H., Bryant, D., 2024. The SplitsTree App: interactive analysis and visualization using phylogenetic trees and networks. Nat. Methods 21, 1773–1774. https://doi.org/10.1038/s41592-024-02406-3.

Jiménez-Moreno, G., Burjachs, F., Expósito, I., Oms, O., Carrancho, Á., Villalaín, J.J., Agustí, J., Campeny, G., Gómez de Soler, B., van der Made, J., 2013. Late Pliocene vegetation and orbital-scale climate changes from the western Mediterranean area. Glob. Planet. Change 108, 15–28. https://doi.org/10.1016/j.gloplacha.2013.05.012.

Kalyaanamoorthy, S., Minh, B.Q., Wong, T.K.F., von Haeseler, A., Jermiin, L.S., 2017. ModelFinder: fast model selection for accurate phylogenetic estimates. Nat. Methods 14, 587–589. https://doi.org/10.1038/nmeth.4285.

Kirschner, J., 1992. Karyological differentiation of *Luzula* sect. Luzula in Europe. Thaiszia 2, 11–39.

Kirschner, J., 1996. *Luzula* sect. *Luzula* (Juncaceae) in Spain. Pl. Syst. Evol. 200, 1–11. https://doi.org/10.1007/BF00984744.

Kirschner, J. (Ed.), 2002. Juncaceae 1: *Rostkovia* to *Luzula*. Species Plantarum: Flora of the World Part 6. National Library of Australia, Canberra, pp. 18–188.

Kirschner, J., 2007. A new species of *Luzula* sect. *Luzula* (Juncaceae) from Costa Rica. Novon 17, 202–205.

Kirschner, J., Křisa, B., 1979. Notes on the taxonomy and cytology of the genus *Luzula* in the West Caucasus. Preslia 51, 333–339.
Leigh, J.W., Bryant, D., 2015. POPART: full-feature software for haplotype network construction. Methods Ecol. Evol. 6, 1110–1116. https://doi.org/10.1111/2041-210X.12410.
Lewis, P.O., 2001. A likelihood approach to estimating phylogeny from discrete morphological character data. Syst. Biol. 50, 913–925.
Linder, C.R., Rieseberg, L.H., 2004. Reconstructing patterns of reticulate evolution in plants. Am. J. Bot. 91, 1700–1708.
Lisiecki, L.E., Raymo, M.E., 2005. A Pliocene-Pleistocene stack of 57 globally distributed benthic δ 18O records. Paleoceanography 20, 1–17.
Luceño, M., Guerra, M., 1996. Numerical variations in species exhibiting holocentric chromosomes: a nomenclatural proposal. Caryologia 49, 301–309. https://doi.org/10.1080/00087114.1996.10797374.
Magulaev, A.Y., 1992. Chromosome numbers in some species of vascular plants of the northern Caucasus flora. Bot. Žhurn. 77, 88–90.
Malinsky, M., Trucchi, E., Lawson, D.J., Falush, D., 2018. RADpainter and fineRADstructure: population inference from RADseq data. Mol. Biol. Evol. 35, 1284–1290. https://doi.org/10.1093/molbev/msy023.
Mata-Sucre, Y., Matzenauer, W., Castro, N., Huettel, B., Pedrosa-Harand, A., Marques, A., Souza, G., 2023. Repeat-based phylogenomics shed light on unclear relationships in the monocentric genus *Juncus* L. (Juncaceae). Mol. Phylogenet. Evol. 189, 107930. https://doi.org/10.1016/j.ympev.2023.107930.
Melters, D.P., Paliulis, L.V., Korf, I.F., Chan, S.W.L., 2012. Holocentric chromosomes: convergent evolution, meiotic adaptations, and genomic analysis. Chromosome Res. 20, 579–593. https://doi.org/10.1007/s10577-012-9292-1.
Miller, M.A., Pfeiffer, W., Schwartz, T., 2010. Creating the CIPRES Science Gateway for inference of large phylogenetic trees. In: 2010 gateway computing environments workshop (GCE). Ieee, pp. 1–8. https://doi.org/10.1109/GCE.2010.5676129.
Minh, B.Q., Schmidt, H.A., Chernomor, O., Schrempf, D., Woodhams, M.D., von Haeseler, A., Lanfear, R., 2020. IQ-TREE 2: New models and efficient methods for phylogenetic inference in the genomic era. Mol. Biol. Evol. 37, 1530–1534. https://doi.org/10.1093/molbev/msaa015.
Müller, K., 2005. SeqState—primer design and sequence statistics for phylogenetic DNA data sets. Appl. Bioinform. 4, 65–69.
Näsvall, K., Boman, J., Höök, L., Vila, R., Wiklund, C., Backström, N., 2023. Nascent evolution of recombination rate differences as a consequence of chromosomal rearrangements. PLoS Genet. 19, e1010717. https://doi.org/10.1371/journal.pgen.1010717.
Nordenskiöld, H., 1951. Cyto-taxonomical studies in the genus *Luzula*. I. Somatic chromosomes and chromosome numbers. Hereditas 37, 325–355. https://doi.org/10.1111/j.1601-5223.1951.tb02898.x.
Nylander, J.A.A., 2004. MrAIC.Pl. Program distributed by the author. Evolutionary Biology Centre, Uppsala University.
Okuyama, Y., Fujii, N., Wakabayashi, M., Kawakita, A., Ito, M., Watanabe, M., Murakami, N., Makoto, K., 2005. Nonuniform concerted evolution and chloroplast capture: heterogeneity of observed introgression patterns in three molecular data partition phylogenies of Asian *Mitella* (Saxifragaceae). Mol. Biol. Evol. 22, 285–296. https://doi.org/10.1093/molbev/msi016.
Ozenda, P., 1985. La végétation de la chaîne Alpine dans l'espace montagnard Européen. Masson, Paris.
Pagel, M., 1999. Inferring the historical patterns of biological evolution. Nature 401, 877–884. https://doi.org/10.1038/44766.
Paradis, E., Schliep, K., 2019. ape 5.0: an environment for modern phylogenetics and evolutionary analyses in R. Bioinformatics 35, 526–528. https://doi.org/10.1093/bioinformatics/bty633.
Pennell, M.W., Eastman, J.M., Slater, G.J., Brown, J.W., Uyeda, J.C., FitzJohn, R.G., Alfaro, M.E., Harmon, L.J., 2014. geiger v2.0: an expanded suite of methods for fitting macroevolutionary models to phylogenetic trees. Bioinformatics 30, 2216–2218. https://doi.org/10.1093/bioinformatics/btu181.
Pungaršek, Š., Dolenc Koce, J., Bačič, M., Barfuss, M.H.J., Schönswetter, P., Frajman, B., 2023. Disentangling relationships among the alpine species of *Luzula* sect. *Luzula* (Juncaceae) in the Eastern Alps. Plants 12, 973. https://doi.org/10.3390/plants12040973.
R Core Team, 2024. R: A language and environment for statistical computing. R Foundation for Statistical Computing, Vienna, Austria. https://www.R-project.org/ (accessed 7 January 2025).
Rambaut, A., 2018. Figtree v. 1.4.4. Institute of Evolutionary Biology, University of Edinburgh, Edinburgh.
Rambaut, A., Drummond, A.J., Xie, D., Baele, G., Suchard, M.A., 2018. Posterior summarisation in Bayesian phylogenetics using Tracer 1.7. Syst. Biol. 67, 901–904. https://doi.org/10.1093/sysbio/syy032.
Revell, L., 2024. phytools 2.0: an updated R ecosystem for phylogenetic comparative methods (and other things). PeerJ 12, e16505. https://doi.org/10.7717/peerj.16505.
Ronquist, F., Teslenko, M., Van Der Mark, P., Ayres, D.L., Darling, A., Höhna, S., Larget, B., Liu, L., Suchard, M.A., Huelsenbeck, J.P., 2012. MrBayes 3.2: Efficient Bayesian phylogenetic inference and model choice across a large model space. Syst. Biol. 61, 539–542. https://doi.org/10.1093/sysbio/sys029.
Schönswetter, P., Suda, J., Popp, M., Weiss-Schneeweiss, H., Brochmann, C., 2007. Circumpolar phylogeography of *Juncus biglumis* (Juncaceae) inferred from AFLP fingerprints, cpDNA sequences, nuclear DNA content and chromosome numbers. Mol. Phylogenet. Evol. 42, 92–103. https://doi.org/10.1016/j.ympev.2006.06.016.
Schönswetter, P., Tribsch, A., Barfuss, M., Niklfeld, H., 2002. Several Pleistocene refugia detected in the high alpine plant *Phyteuma globulariifolium* Sternb. & Hoppe (Campanulaceae) in the European Alps. Mol. Ecol. 11, 2637–2647. https://doi.org/10.1046/j.1365-294X.2002.01651.x.
Simmons, M.P., Ochoterena, H., 2000. Gaps as characters in sequence based phylogenetic analyses. Syst. Biol. 49, 369–381.
Smith, T.W., Kron, P., Martin, S.L., 2018. flowPloidy: an R package for genome size and ploidy assessment of flow cytometry data. Appl. Plant Sci. 6, e01164. https://doi.org/10.1002/aps3.1164.
Soltis, D.E., Visger, C.J., Blaine Marchant, D., Soltis, P.S., 2016. Polyploidy: pitfalls and paths to a paradigm. Am. J. Bot. 103, 1146–1166. https://doi.org/10.3732/ajb.1500501.
Španiel, S., Rešetnik, I., 2022. Plant phylogeography of the Balkan Peninsula: spatiotemporal patterns and processes. Plant Syst. Evol. 308, 38. https://doi.org/10.1007/s00606-022-01831-1.
Steckenborn, S., Marques, A., 2025. Centromere diversity and its evolutionary impacts on plant karyotypes and plant reproduction. New Phytol. 245, 1879–1886. https://doi.org/10.1111/nph.20376.
Suc, J.-P., Zagwijn, W.H., 1983. Plio-Pleistocene correlations between the northwestern Mediterranean region and northwestern Europe according to recent biostratigraphic and palaeoclimatic data. Boreas 12, 153–166. https://doi.org/10.1111/j.1502-3885.1983.tb00309.x.
Suc, J.P., 1984. Origin and evolution of the Mediterranean vegetation and climate in Europe. Nature 307, 429–432.
Suda, J., Trávníček, P., 2006. Estimation of relative nuclear DNA content in dehydrated plant tissues by flow cytometry. Curr. Prot. Cytom. 38, 7.30.1-7.30.14. https://doi.org/10.1002/0471142956.cy0730s38.
Tel-Zur, N., Abbo, S., Myslabodski, D., Mizrahi, Y., 1999. Modified CTAB procedure for DNA isolation from epiphytic cacti of the genera *Hylocereus* and *Selenicereus* (Cactaceae). Plant Mol. Biol. Rep. 17, 249–254. https://doi.org/10.1023/A:1007656315275.
Tribble, C.M., Márquez-Corro, J.I., May, M.R., Hipp, A.L., Escudero, M., Zenil-Ferguson, R., 2024. Macroevolutionary inference of complex modes of chromosomal speciation in a cosmopolitan plant lineage. New Phytol. 245, 2350–2361. https://doi.org/10.1111/nph.20353.
Wendel, J.F., Doyle, J.J., 1998. Phylogenetic incongruence: window into genome history and molecular evolution. In: Soltis, P., Soltis, D., Doyle, J. (Eds.), Molecular Systematics of Plants II. Kluwer Academic Press, Dodrecht, pp. 265–296.
Záveská Drábková, L., Vlček, Č., 2009. DNA variation within Juncaceae: comparison of impact of organelles regions on phylogeny. Plant Syst. Evol. 278, 169–186. https://doi.org/10.1007/s00606-008-0135-7.
Záveská Drábková, L., Vlček, Č., 2010. Molecular phylogeny of the genus *Luzula* DC. (Juncaceae, Monocotyledones) based on plastome and nuclear ribosomal regions: a case of incongruence, incomplete lineage sorting and hybridisation. Mol. Phylogenet. Evol. 57, 536–551. https://doi.org/10.1016/j.ympev.2010.07.022.
Zedek, F., Bureš, P., 2018. Holocentric chromosomes: from tolerance to fragmentation to colonization of the land. Ann. Bot. 121, 9–16. https://doi.org/10.1093/aob/mcx118.
Zedek, F., Bureš, P., Elliott, T.L., Escudero, M., Lucek, K., Marques, A., 2025. Chromosome size as a universal predictor of recombination rate: insights from holocentric and monocentric systems. bioRxiv. https://doi.org/10.1101/2025.07.10.664216.

Further reading

Kirschner, J., 1991. An account of natural hybridization within *Luzula* sect. *Luzula* (Juncaceae) in Europe. Preslia 63, 81–112.